PROCESS PARAMETER OPTIMIZATION OF URBAN BIOWASTE CARBONIZATION

Sinhara Mudalige Hasitha Dhananjana Perera
(159261R)

Dissertation submitted in partial fulfillment of the requirements for the degree Master of Science

Department of Chemical and Process Engineering

University of Moratuwa
Sri Lanka

January 2020

DECLARATION

I declare that this is my own work and this dissertation does not incorporate without acknowledgment any material previously submitted for a Degree or Diploma in any other University or institute of higher learning and to the best of my knowledge and belief it does not contain any material previously published or written by another person except where the acknowledgment is made in the text.

Also, I hereby grant to University of Moratuwa the non-exclusive right to reproduce and distribute my dissertation, in whole or in part in print, electronic or other medium. I retain the right to use this content in whole or part in future works (such as articles or books).

…… ……..

Signature Date

The above candidate has carried out research for the Masters Dissertation under my supervision.

…… …….

Signature of the supervisor Date

Prof. Mahinsasa Narayana
Department of Chemical and Process Engineering,
University of Moratuwa.

ABSTRACT

About 75% of Municipal solid waste (MSW) collected around the country is organic biomass which mainly includes food waste, wood, paper, saw dust and paddy husk. Urban councils in Colombo city and nearby suburbs collect biowaste separately which has created a huge potential in converting urban biowaste into value-added component like biochar, thus resolving the problems associated with MSW management and mitigating socio-economic and environmental issues related to MSW. In this study, torrefaction is identified as the most viable technology available for the conversion of organic MSW into biochar and the study mainly focuses on developing a three dimensional computational fluid dynamics (CFD) model of a continuous packed-bed torrefaction reactor for organic MSW and then optimizing the process variables and the geometry. A mathematical model including all heat, mass and energy transfers, and heterogeneous & homogeneous reactions is firstly developed and then converted to a numerical model and simulated using OpenFOAM for an insulated cylindrical reactor in which hot gas at elevated temperatures (473 – 623K) is provided from the bottom while solid at ambient conditions is fed from the top. The torrefaction reactor is optimized for gas inlet temperature and residence time and then the geometry of the reactor is optimized for the optimum gas inlet temperature and residence time. Four reaction zones are identified in the reactor domain; i.e. drying, softening & depolymerization, limited devolatilization & carbonization and extensive devolatilization and carbonization. The optimum inlet gas temperature, residence time and D/L ratio are 573K, 13000s and 0.24 respectively. For the optimum conditions, biochar yield is 55.7% while ash content is 19.1%. Further In dry basis, 95.9% of biomass is decomposed and the total weight loss based on the initial wet biomass is 86.6%.

Keywords: Urban biowaste; Biochar; Torrefaction; Computational fluid dynamic; Continuous packed-bed; numerical model

ACKNOWLEDGMENT

I owe my deepest gratitude to the people mentioned below without whom the successful completion of this research would not have been possible. The support received in numerous ways is invaluable and beyond description.

First and foremost, I would like to express my heartfelt gratitude to my supervisor Prof. Mahinsasa Narayana for the immense support and the technical guidance provided throughout the course of conduction of this research. His immense knowledge and vast experience in the field of modeling and simulation helped me tremendously whenever I had come across with problems. Also I am very much grateful for the inspiration and motivation given by him to accelerate the research activities whenever I was lagging behind the schedule.

It is with great pleasure that I acknowledge Mr. Chathuranga Wikramasinghe for the tremendous support given throughout the research. I am indebted to him for the assistance provided during the learning process of C++ language and OpenFOAM software. Also I owe my gratitude to him for the support given in finding resource materials.

I gratefully acknowledge all the lecturers of Department of Chemical and Process Engineering, University of Moratuwa. Also I would like to extend my gratitude to non-academic staff of Department of Chemical and Process Engineering, University of Moratuwa. Further I would like to specially thank Mr. Sunil Dayananda of Process Control Laboratory of Department of Chemical and Process Engineering for facilitating laboratory resources.

All the colleagues supported me during the course of conduction of this research are earnestly remembered for their numerous support. Finally I would like to express my heartfelt gratitude to my beloved family for motivating me to complete this research successfully.

TABLE OF CONTENTS

LIST OF FIGURES

LIST OF TABLES

LIST OF ABBREVIATIONS

Abbreviation	Description
CFD	Computational Fluid Dynamics
MSW	Municipal Solid Waste

LIST OF APPENDICES

NOMENCLATURE

ρ_g - Density of gas phase (kg m^{-3})

ϵ_g - Volume fraction of gas phase

U_g - Velocity of gas phase (m s^{-1})

μ - Dynamic viscosity (Pa s)

p - Pressure (Pa)

k - Turbulent kinetic energy (m^2 s^{-2})

I - Second order identity tensor

d - Particle size (m)

T_g - Gas phase temperature (K)

T_s - Solid phase temperature (K)

ρ_s - Density of solid phase (kg m^{-3})

ϵ_s - Volume fraction of solid phase

$C_{v,g}$ - Specific heat capacity of gas phase (J kg^{-1} K^{-1})

C_s - Specific heat capacity of solid phase (J kg^{-1} K^{-1})

k_g - Thermal conductivity of gas phase (W m^{-1} K^{-1})

k_s - Thermal conductivity of solid phase (W m^{-1} K^{-1})

$R_{i,hetero}$ - Rate of heterogeneous reaction i (kg m^{-3} s^{-1})

$R_{i,homo}$ - Rate of homogeneous reaction i (kg m^{-3} s^{-1})

Q_R - Radiation heat (W)

h - Heat transfer coefficient (W m^{-2} K^{-1})

A - Specific surface area of bed (m^{-1})

ΔH_i - Enthalpy of the reaction i (J kg^{-1})

$Y_{g,i}$ - Mass fraction of i in the gas phase

$Y_{s,i}$ - Mass fraction of i in the solid phase

$D_{g,i}$ - Diffusion coefficient of i in the gas phase (m^2 s^{-1})

$D_{s,i}$ - Diffusion coefficient of i in the solid phase (m^2 s^{-1})

r_{cel} - Degradation rate of cellulose (kg m^{-3} s^{-1})

r_{hem} - Degradation rate of hemicellulose (kg m^{-3} s^{-1})

r_{lig} - Degradation rate of lignin (kg m^{-3} s^{-1})

f_{cel} - Pre-exponential factor of cellulose decomposition (s^{-1})

f_{hem} - Pre-exponential factor of hemicellulose decomposition (s^{-1})

f_{lig} - Pre-exponential factor of lignin decomposition (s^{-1})

E_{cel} - Activation energy of cellulose decomposition (kJ mol^{-1})

E_{hem} - Activation energy of hemicellulose decomposition (kJ mol^{-1})

E_{lig} - Activation energy of lignin decomposition (kJ mol^{-1})

Y_{cel} - Mass fraction of cellulose

Y_{hem} - Mass fraction of hemicellulose

Y_{lig} - Mass fraction of lignin

$r_{k,O2}$, $r_{k,CO2}$ and $r_{k,H2O}$ - Kinetic reaction rate of char combustion, char CO_2 gasification and char H_2O gasification respectively (kg m^{-3} s^{-1})

f_{O2}, f_{CO2} and f_{H2O} - Pre-exponential factor of char combustion, char CO_2 gasification and char H_2O gasification respectively (m s^{-1} K^{-1})

E_{O2}, E_{CO2} and E_{H2O} - Activation energy of char combustion, char CO_2 gasification and char H_2O gasification respectively (kJ mol^{-1})

M_c, M_{O2}, M_{CO2} and M_{H2O} - Molar mass of char, O_2, CO_2 and H_2O respectively (kg mol^{-1})

v_{O2}, v_{CO2} and v_{H2O} - Stoichiometric coefficient of O_2, CO_2 and H_2O in char combustion, char CO_2 gasification and char H_2O gasification reactions respectively

ρ_{O2}, ρ_{CO2} and ρ_{H2O} - Density of O_2, CO_2 and H_2O in the gas phase respectively (kg m^{-3})

m_{char} - Mass of char per unit volume (kg m^{-3})

$m_{biomass}$ - Initial mass of biomass per unit volume (kg m^{-3})

a - Average stoichiometric coefficient of char in the degradation reactions

A_{ss} - Total specific surface area of solid phase (m^2)

$r_{m,O2}$, $r_{m,CO2}$ and $r_{m,H2O}$ - Mass transfer rate of O_2, CO_2 and H_2O (kg m^{-3} s^{-1})

$\rho_{O2,s}$, $\rho_{CO2,s}$ and $\rho_{H2O,s}$ - Density of O_2, CO_2 and H_2O in the solid surface respectively (kg m^{-3})

$k_{m,O2}$, $k_{m,CO2}$ and $k_{m,H2O}$ - Mass transfer coefficient of O_2, CO_2 and H_2O respectively (m s^{-1})

Sh_i - Sherwood number of i^{th} gas

Sc_i - Schmidt number of i^{th} gas

$D_{i,g}$ - Diffusion coefficient of i^{th} gas ($m^2\ s^{-1}$)

Re - Reynolds number

$r_{k,i}$ - Kinetic reaction rate of i^{th} equation (kmol $m^{-3}\ s^{-1}$)

f_i - Pre-exponential factor of i^{th} equation

E_i - Activation energy of i^{th} equation (kJ mol^{-1})

$[H_2], [O_2], [CO], [H_2O], [CO_2]$and $[CH_4]$ - Concentration of H_2, O_2, CO, H_2O, CO_2 and CH_4 in the gas phase (kmol m^{-3})

$r_{t,i}$ - Turbulent mixing limited reaction rate (kmol $m^{-3}\ s^{-1}$)

ρ_g - Density of gas (kg m^{-3})

k - Turbulent kinetic energy ($m^2\ s^{-2}$)

$\in$ - Turbulent dissipation rate ($m^2\ s^{-3}$)

Y_j and Y_k - Mass fraction of reactants of reaction i

v_j and v_k - Stoichiometric metric coefficient of reactants of reaction i

M_j and M_k - Molar mass of reactants of reaction i (kg $kmol^{-1}$)

Q_{sg} - Interphase convective heat transfer rate (W)

A - Specific surface area of solid (m^{-1})

Nu - Nusselt number

Re - Reynolds' number

Pr - Prandtl number

G - Incident intensity (W m^{-2})

a - Absorption coefficient of gas phase (m^{-1})

a_p - Absorption coefficient of solid phase (m^{-1})

n - Refractive index of gas phase

σ - Stefan constant (W $m^{-2}\ K^{-4}$)

E_p - Equivalent emission of particles

A_r - Specific surface area available for radiation (m^{-1})

ε - Emissivity of solid particles

H_{evp} - Heat of evaporation (kJ $kg^{-1}\ m^{-3}$)

$Y_{moisture}$ - Mass fraction of moisture

r_d - Drying rate (kg $m^{-3}\ s^{-1}$)

E_{tor} - Torrefaction heat (kJ m^{-3})

$C_{v,g}$ - Specific heat of gas (kJ K^{-1} kg^{-1})

$R_{biomass}$ - Decomposition rate of biomass (kg m^{-3} s^{-1})

E_{Ri} - Energy released or absorbed due to the reaction i (kJ m^{-3})

r_i - Rate of the reaction i (kmol m^{-3} s^{-1})

H_i - Enthalpy of the reaction I (kJ mol^{-1})

1. INTRODUCTION

In today's world, energy and waste management are two most critical aspects of industry and environment which have been the major deciding factors of the global socio-economic and environmental future. In the process of finding solutions for global energy crisis and environmental pollution, many researches in various scales have been conducted on biomass and thus it is well-identified as a potential candidate for ever-rising energy demand and also as a major solution in waste management which can mitigate environmental pollution up to a greater extent.

1.1 Biomass

Biomass is solid matter derived through natural biological processes. In other words, it stands for all organic materials which include the land and water-based vegetation such as trees, crops and algae, and also all organic waste. As a result of many studies scrutinized on extracting energy stored in biomass as chemical bond energy formed between Carbon, Hydrogen and Oxygen through the photosynthesis by absorbing solar energy, it has been identified that reverse process of breaking those bonds and emission of energy is possible via thermochemical and biological processes such as combustion, digestion and decomposition [1]**.** Thus biomass is on the spotlight as the 21st century major renewable energy source which is expected to cater for 50% of the total primary energy demand in future. In fact biomass (traditional biomass) was dominating as a major energy source in the past before the 20th century, which is clearly explained by historical energy statistics and it gradually restricted to domestic applications in rural areas over the time with the introduction of fossil fuels to the energy market [2]. But with the awareness of fossil fuel depletion and its associated drawbacks such as market price fluctuations as well as environmental concerns such as Carbon footprint, attraction towards renewable sustainable energy sources emerged in the beginning of this new millennium thus leading to numerous studies and researches on use of biomass effectively in energy application without restricting to its traditional usage.

According to the global bioenergy statistics of World Bioenergy Association, renewables have contributed by 18% to gross energy consumption globally in 2016. Further 13% out of 18% of renewable energy, which is equal to 72% of total renewable energy, was contributed by biomass [3].

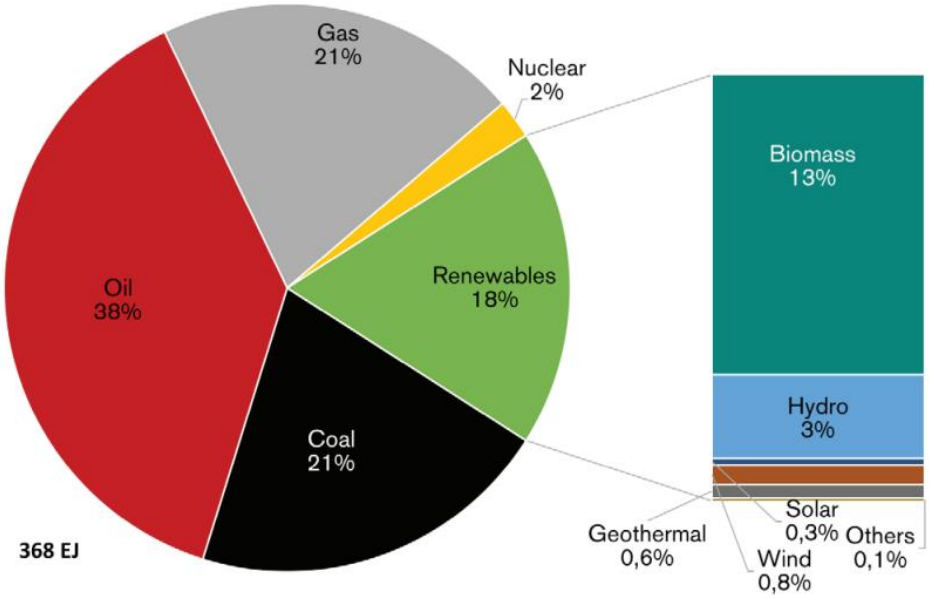

Figure 1-1: Gross final energy consumption globally in 2016 [3]

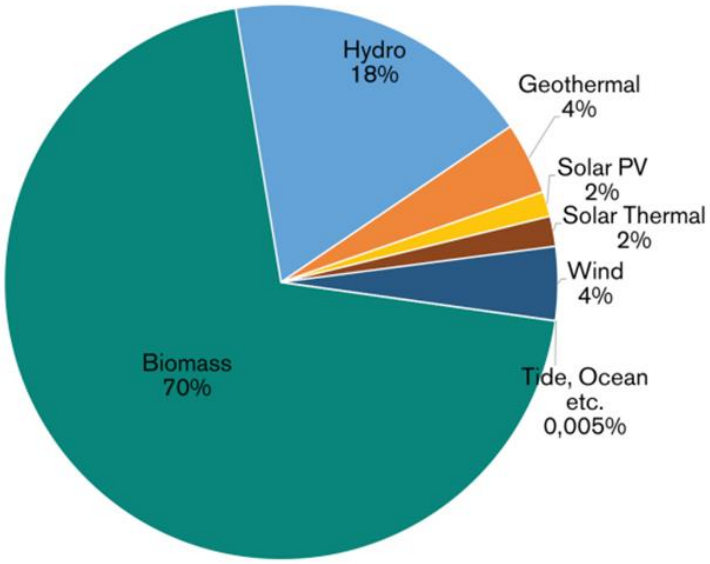

Figure 1-2: Total primary energy supply of all renewables in 2014 [3]

1.2 Potential of biomass in waste management

At present, generation of solid waste which is influenced by several factors such as geographical location, economic development, energy sources, cultural norms and climate, is estimated to be around 1.3 billion Tons per year globally and waste generation rate is forecasted to be more than double throughout the next two decades in which global waste generation is expected to rise to 2.2 billion Tons by 2025 [4]. As with the rapid urbanization, waste generation is racing and unfortunately most of solid waste goes into landfills causing serious social, economic and environmental issues.

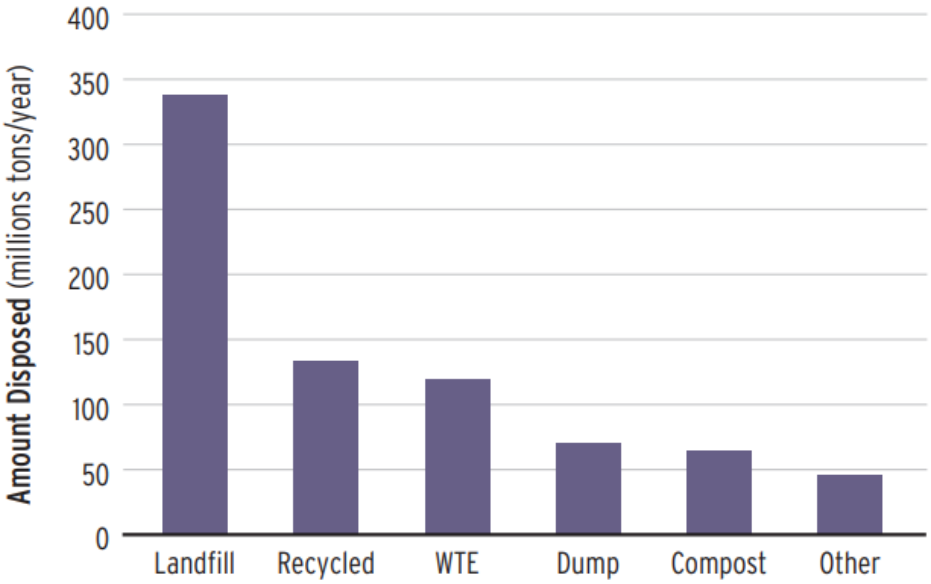

Figure 1-3: Total MSW disposed of worldwide [4]

In order to highlight some burning issues, followings can be mentioned.

- Increased greenhouse gas emission due to methane gas emissions from waste in landfills and open combustion of waste.
- Air, water and soil pollution due to the waste contamination.

- Health and sanitary issues arising from exposing to contaminated air, water and food.
- Huge financial cost associated with waste management. (Total global waste management cost is estimated to be $205.4 billion) [4].
- Wasted land for landfills which otherwise could have been used productively in agricultural or commercial applications.

Most of the solid waste generated globally is organic waste. In fact, nearly 50% of the total solid waste generated accounts for organic waste (biomass) which can be effectively utilized in waste to energy (WTE) techniques and waste to value-added components such as fertilizer and biochar or combination of both.

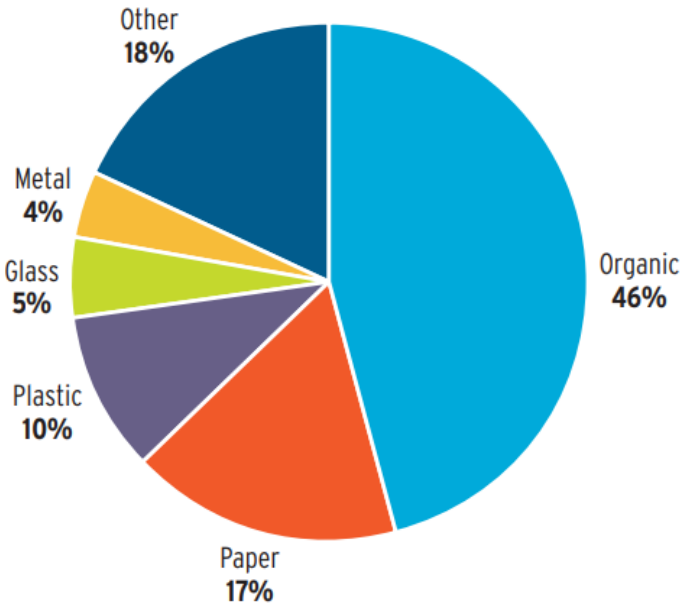

Figure 1-4: Global solid waste composition [4]

Most of WTE technologies associated with thermochemical processes are with lesser operational and capital cost and top of everything biowaste is for free and is available in large quantities. Ultimately troublesome biowaste which is half of the total solid waste can be effectively converted to energy or value added fertilizer like components which have a reasonable economic value by which it is able to cover up the waste management

cost for some extent and mitigate the environmental pollution for greater extent. Further, quantities of wasted residue generating from these processes are minimal and require lesser space in landfills.

1.3 Context of municipal solid waste in Sri Lanka

Municipal solid waste (MSW) is heterogeneous collection of wastes which include all the types of domestic and institutional waste such as schools, businesses, and hospitals etc. It is disposed daily basis and is collected in regular intervals by local government councils. According to the local government act of Sri Lanka, all the municipal waste collected by local authorities is legally considered to be a property of councils and they are responsible in disposing, processing and recycling MSW safely in a manner such that it ensures environmental accountability and social responsibility. Currently in Sri Lanka, MSW is collected by 23 municipal councils, 41 urban councils and 271 "Pradeshiya Sabhas". Following given is the average solid waste generation in Sri Lankan local government councils [5].

Table 1-1: Average per capita per day waste generation in Sri Lankan local government councils [5]

Local Authority	Quantity per capita (kg/day)
Colombo MC	0.80
Other MC's	0.65 - 0.80
Urban Councils	0.45 - 0.65
Pradeshiya Sabhas	0.20 - 0.45

According to Central Environmental Authority, Solid waste generation in 2001 in Sri Lanka is approximately 6400 tons per day and composition of MSW collected as per the given table 1-2 [5].

Table 1-2: Average composition of MSW collected in Sri Lanka [5]

Component	Percentage
Biodegradable (ST)	56.57%
Biodegradable (LT)	5.94%
Paper	6.47%
Wood	6.35%
Saw dust/Paddy husk	6.04%
Polythene/Plastic	5.91%
Building	3.89%
Metal	2.76%
Slaughter house	2.34%
Glass	2.03%
Other	1.68%

About 75% of total MSW generated is biomass and can be utilized in WTE projects and composting or biochar generation which will reduce the total weight tremendously while providing useful energy or value-added components like fertilizer and biochar. Nevertheless Sri Lanka still struggles to manage MSW and lacks proper waste management programme thus leading to serious environmental issues and disasters such as Meethotamulla landslide. Most of MSW generated goes into open dumps while lesser portion is managed in semi-controlled landfills in which source separated MSW is consumed in recycling and composting. At present, country only has single sanitary landfill which is located in Dompe, Gampaha district.

1.4 Organic waste processing technologies

Biomass is productively processed to generate heat, electricity, combined heat & electricity, fertilizer, biochar and bio-oil. In that purpose, there exists a wide range of technologies which are mainly categorized into thermal, thermochemical, biological and biochemical processes such as pyrolysis, gasification incineration, torrefaction, fermentation, anaerobic digestion, hydrothermal carbonization [6].

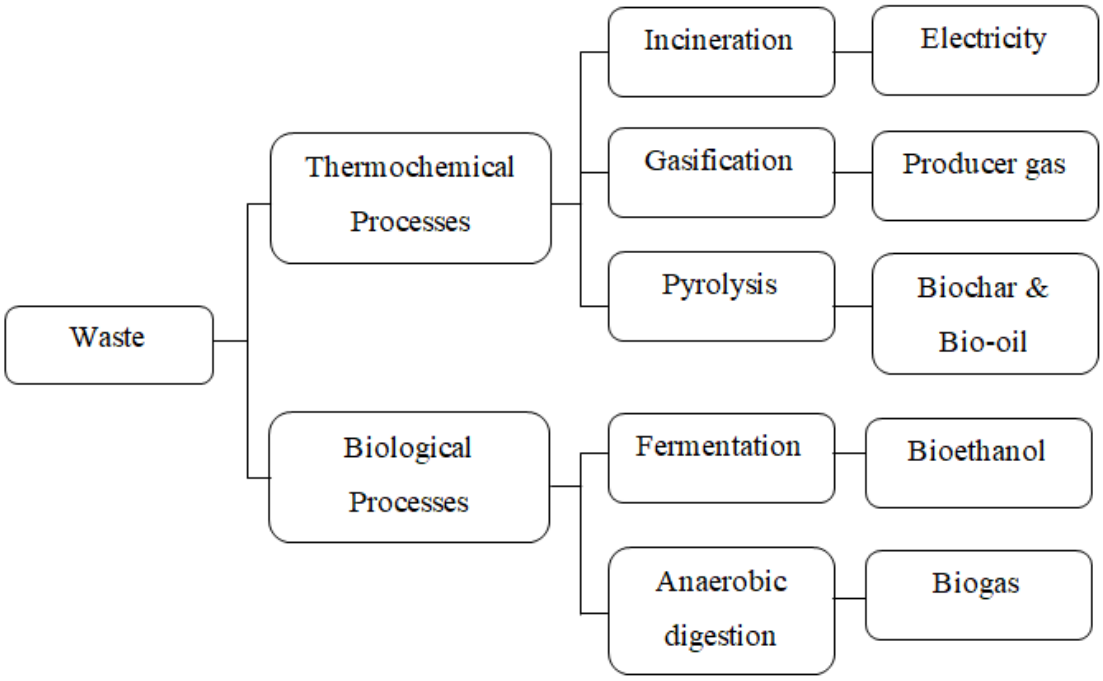

Figure 1-5: Biowaste processing technologies

1.4.1 Gasification

Gasification is the process of incomplete combustion of biomass in a limited oxygen environment, which results a mixture of combustible gases consisting of methane, hydrogen, carbon monoxide and carbon dioxide, which is also known as producer gas and it is used to produce heat and power in boilers, turbines and engines. This is a two-stage process where the first is pyrolysis in which volatile gases and char are generated,

is followed by gasification where char is further reacted with steam or limited oxygen to produce combustible gases. In industry, there are two main categories of gasifiers which are known as fixed bed and fluidized bed gasifiers [7].

1.4.2 Pyrolysis, Torrefaction and Incineration

Pyrolysis is the thermal decomposition of biomass at elevated temperatures in an oxygen free environment and it produces biochar, bio-oil and combustible gases. If this pyrolysis process is carried out at a relatively low temperature less than 450 ^{0}C, biochar generation is increased significantly. Pyrolysis process at relatively low temperatures and longer residence times is called torrefaction and it produces high yield of biochar while generating heat and combustible gases. This process reduces the volume of biowaste tremendously and produced biochar is a value-added product which can be used in diverse range of applications [8]. In contrast to the gasification technology where primary objective is to maximize the conversion of biomass into combustible gas, in torrefaction (slow pyrolysis), the aim is to increase the biochar yield.

Incineration is the simplest combustion process of biomass and is carried out in a closed environment which converts biomass into heat, flue gas and ash. This flue gas is required to be purged before it is released into atmosphere. Incineration reduces the volume of waste tremendously while producing valuable heat and energy which can be exploited in various energy applications.

1.4.3 Fermentation, Anaerobic digestion and Hydrothermal carbonization

Fermentation and anaerobic digestion are the most widely used biochemical conversion technologies of biomass which involve microorganisms and enzymes to breakdown biomass into liquid and gaseous fuel. In anaerobic digestion, biomass is decomposed by metabolic activities of microorganisms in an oxygen depleted environment [9]. These biochemical processes are more effective in processing wet organic waste or waste with high moisture content since huge amount of energy is required to evaporate moisture in thermochemical processes.

Hydrothermal carbonization is a thermal conversion technology which is used to process wet biomass into energy and hydrochar at self-generated pressures in subcritical water. Similar to the torrefaction process, primary objective of this process is to maximize the char yield which is decided based on several factors such as temperature, heating rate, aqueous quality, reactant concentration and residence time [10].

1.5 Background of the research

As with the economic growth and rapid urbanization of the country, MSW generation is escalating over the years without proper waste management system. As a result, Sri Lanka is now facing serious social, economic and environmental issues. Garbage heaps are elevating like skyscrapers of the city causing a serious threat to people and environment. There is no guarantee that tragic incident like Meethotamulla which cost 32 human lives, will not happen again. At present, country's main waste disposal method is open dumping while there are few semi-controlled landfills and a single sanitary landfill [11]. The impact of open dumping on environment and socio-economic development is devastating and some serious issues are highlighted below,

- Contamination of ground water with leachate of landfills and also surface water in rainy seasons which leading to serious health issues.
- Intense greenhouse gas emission and air pollution. People who reside near dump sites are affected by smelling which is carried away by wind.
- Insects and rodent infestations and accelerated spreading of diseases caused by viruses and bacteria.
- Due to insufficient landfills, new dump sites are created in rural environmental sensitive areas escalating the issue further. Some wild animals consume garbage and put their lives at risk due to plastic and polythene materials in the garbage.

About 75% of the total MSW generated in the country is biomass and can be processed using WTE technologies. Energy and value-added solid products such as biochar are

yielded from biowaste and it minimizes the volume of solid waste that is going into landfills. In fact, a total solution for the 75% of MSW can be achieved, if the biowaste is converted to energy and biochar combined with small percentage of ash and other impurities.

In Sri Lankan Context, Carbonization of biowaste is the most promising method to mitigate the problem of MSW. Through the carbonization of organic waste, the main output is biochar which has diverse range applications, and as a result of production of value-added component like biochar, cost of management and operation will be compensated thus leading to an economically viable waste management system. Gas generated during the carbonization process can be recycled back to the reactor to provide the required heat thus making the process self-sufficient with energy.

There are two available thermochemical technologies of carbonization which are torrefaction (slow pyrolysis) and hydrothermal carbonization. Former is more suitable for solid waste while latter is effective with liquid organic waste. Torrefaction of organic waste produces a high yield of biochar compared to other processes such as gasification and pyrolysis. Biochar has various applications and few important ones are mentioned below.

- Mixing material for landfill capping.
- Phytocapping of dumps (this minimizes the greenhouse and toxic volatile organic gas emissions).
- For permeable reactive barriers and leachate treatment.
- In fertilizer production (hybrid fertilizer can be produced mixing biochar with compost).

Through effectively managed torrefaction process of organic waste, Sri Lanka is very much capable to achieve a socio-economically viable and financially sustainable solid waste management system.

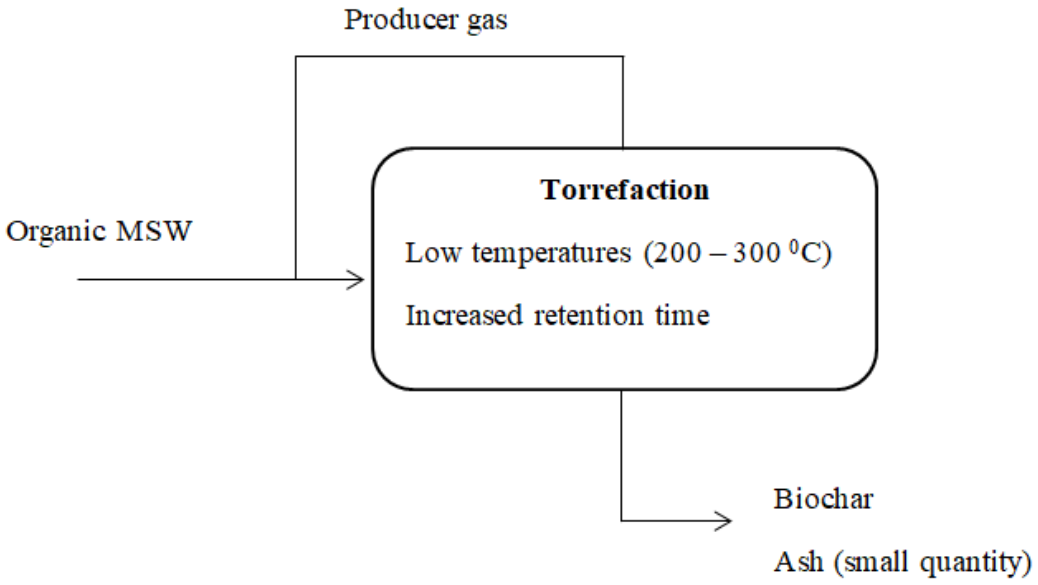

Figure 1-6: Organic waste torrefaction

1.6 Research problem

Core of the torrefaction process of organic waste is the torrefaction reactor and design of the reactor significantly affect the yield and quality of biochar, physical characteristics such as particle size, porosity, density and structure, moisture content, ash content, maximum bed temperature and temperature & composition of flue gas. Hence the success of torrefaction process is mainly dependent on a well-designed and optimized reactor. Optimization of the torrefaction reactor plays a key role in whole process of conversion of organic MSW to biochar via torrefaction and it will decide the productivity of torrefaction process and the quality of biochar produced. Depending on the quality and physical characteristics of biochar produced, its applications will differ.

Optimization of the torrefaction reactor can be carried out in two ways; i.e. computer aided modelling & simulation and experiments. Experimental approach in optimization involves series of manual experiments in both laboratory and pilot scale, which has various difficulties and drawbacks as given below [12] [13].

- High cost associated with fabricating and modifying laboratory scale prototypes and pilot-scale reactors.
- Practically optimization can only be performed for limited number of variables and finite number of data points.
- Experimental procedures are time-taking and expensive.
- Geometry optimization is a tedious task due to the time and cost utilized in designing, fabricating and modifying laboratory scale and pilot-scale reactors.
- Scaled-down laboratory scale reactors and its results may not completely agree with pilot-scale reactors due to the incompatibilities of particle geometries and vessel geometries, which may result inaccuracies leading to hectic trial and error routines.

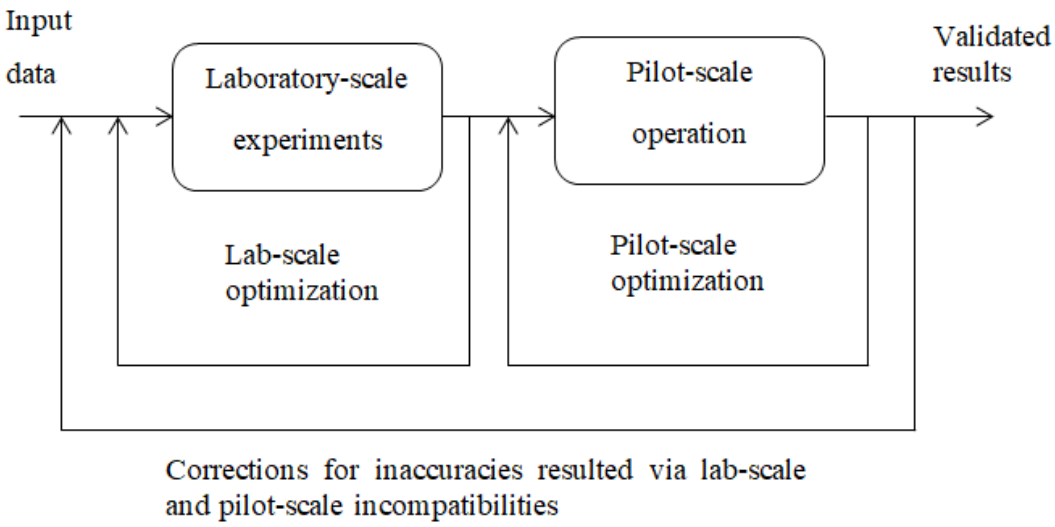

Figure 1-7: Experimental approach in optimization

On the other hand, computer-aided modelling & simulation makes the optimization lot easier eliminating most of drawbacks and inaccuracies in conventional experimental mechanisms. Depending on the computational capacities available, optimization can be carried out for many variables simultaneously in very short time compared to manual experiments. Followings are some of the major advantages in computer-based approach of optimization [14] [15].

- Only the initial capital cost for computer hardware and software and no cost for repeating optimization. In fact, optimization can be done as many times as required with no cost.
- Optimization can be done for huge number of variables simultaneously and complete variations of variable profiles over any geometrical region of interest in various complexities with respect to time can be received.
- Less time consuming depending on the computer hardware capacity.
- Easy to perform geometrical optimization for any complex geometry.
- Computer-aided modelling and simulation of reactors is usually carried out for scale-up dimensions of actual operation.
- Freedom to change any input parameter or variable at will, and analyse the results.

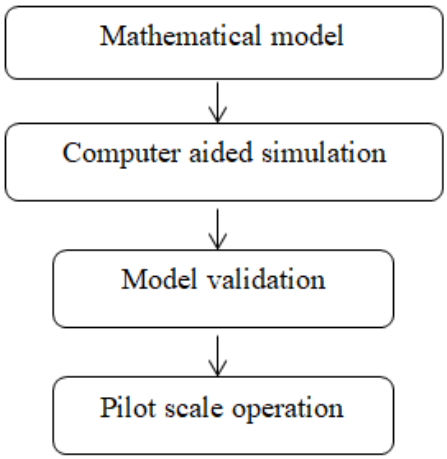

Figure 1-8: Computer-aided simulation and optimization

Perfect optimization is possible to achieve for comparatively very less cost via computer-aided simulation and success of the process mainly depends on the mathematical model developed for the actual process. The more mathematical model agrees with the actual process, the higher accuracy of the simulation gets.

Once the mathematical model of process is ready, it is required to be converted into computable numerical algorithms. Then these algorithms are coded by secondary

languages incorporated in computational fluid dynamics software and is subsequently converted to the machine language where by numerical solutions is achieved.

1.6.1 Modelling and simulation of organic waste torrefaction using CFD

Computational fluid dynamic or in short CFD, is the computer-based numerical analysis of systems which are associated with fluid flow, heat & mass transfer, chemical reactions and other types of transport phenomena. CFD is a very sophisticated technique and is used in various fields of engineering applications such as chemical and process engineering, environmental engineering, biomedical engineering, marine engineering, aerospace engineering, hydrology, oceanography, meteorology and civil engineering. It has gained a vast popularity in engineering optimization of systems due to above mentioned unique advantages in page 13 and its ability to analyse systems where controlled experiments are difficult and beyond the safe operational limits [16].

Torrefaction process of organic waste includes solid and gas phase heat and momentum transfer, gas-phase homogeneous reactions and solid & gas phase heterogeneous reactions. All these phenomena can be readily simulated using CFD techniques.

1.6.2 Introduction to OpenFOAM

There are many CFD software available such as OpenFOAM, ANSYS Fluent, PowerFLOW, Autodesk CFD and FLOW-3D etc. OpenFOAM which is developed by OpenCFD Ltd is one of the very sophisticated and freely available CFD software which is coded in C++ language. It can be installed and used in both Linux and Widows operating systems. Top of everything, in OpenFOAM, user can freely develop and modify customized solvers which are unique to specific applications and there are thousands of inbuilt libraries which can be readily modified according to the application. Further it has wide variety of inbuilt solvers for different applications such as compressible flow, incompressible flow, non-Newtonian flow and chemical reactions etc.

In the course of this research, primary focus is to simulate and optimize a reactor for torrefaction of composted organic MSW. Considering uniqueness of the process, it is required to customize a unique solver and hence OpenFOAM is selected in the process of modeling and simulation of torrefaction reactor.

1.7 Scope of the research

In Sri Lanka, total MSW generation is around 6400 Tons per day and about 59% of the total MSW is generated in the Western province. Further 44% of the total MSW is accounted for Colombo district and that explains severity of solid waste related socio-economic and environmental issues in Colombo city and suburbs. At presents, After Meethotamulla dump site being closed down, the main landfill site which takes the highest MSW intake in Colombo district is located in Karadiyana, Piliyanda [5]. It takes MSW from five highest MSW generating municipal councils after Colombo municipal council; i.e. Maharagama, Dehiwala, Moratuwa, Boralasgamuwa and Kesbewa. One positive occurred in the last two-year time period is that municipal councils in Colombo district collect biowaste separately.

About 75% of MSW generated in above mentioned municipal councils which comes into Karadiyana landfill is organic waste thus creating a great potential in conversion of waste to energy or value-added components. Currently, there is a composting plant at Karadiyana which processes most of the organic waste received into compost fertilizer by aerobic digestion. However, the compost mixture produced lacks quality for it to be marketed as fertilizer. Nevertheless, this compost mixture can easily be converted into biochar by slow pyrolysis or torrefaction and this will improve the value addition tremendously. The biochar produced in such manner, is rich in fixed carbon and can be used in various applications such as manufacture of fertilizer and leachate absorbent.

In the torrefaction process of composted organic MSW, productivity and quality of biochar produced lies upon a well-optimized reactor. Omitting all types of practical difficulties and most importantly the huge cost associated with the experimental

optimization approach in this kind of community project, computer-aided modelling and simulation boast its superiority in all factors such as accuracy, time, cost and repeatability in other similar applications.

In the course of this research, development of accurate mathematical model for torrefaction of compost mixture yielded from aerobic digestion of organic MSW at Karadiyana landfill site, is firstly focused. Computation fluid dynamics (CFD) is an excellent tool to model and simulate this kind of process which is having momentum, mass and heat transfer as well as both homogeneous and heterogeneous reactions. In this purpose, OpenFOAM version 7.0 is employed considering that it is free of charge and allows unlimited access to customized solvers. Once the mathematical model is ready, it is to be coded into numerical algorithms using OpenFOAM and then the simulations will be carried out for variable optimization including temperature and residence time, and also for reactor geometry optimization.

1.8 Research objectives

- Study the thermochemical process of the torrefaction for biochar production
- Development of mathematical model for the torrefaction process of composted organic MSW.
- Developing OpenFOAM cases to simulate the reactor for actual torrefaction process of composted organic MSW.
- Optimization of the torrefaction process parameters and reactor geometry.

1.9 Thesis outline

The research work and its findings are elaborated in this dissertation section by section in which it begins with the introduction as the first chapter where it discusses the background of the research including current trends in biomass technology, global and local municipal solid waste statistics and its associated socio-economic and environmental impacts, biomass processing technologies, most effective commercially

viable biomass conversion technology in the context of Sri Lankan MSW, how torrefaction of composted organic MSW can be applied to successfully manage Karadiyana landfill site and application of computational fluid dynamics technique in optimization of torrefaction process of composted organic MSW.

In the second chapter, comprehensive literature review is presented in details on technical aspects of torrefaction including reaction mechanisms, chemical kinetics and thermodynamics. In the latter part of the chapter, CFD approach in modelling including finite volume method and numerical schemes used in pressure-velocity coupling is discussed.

Study methodology of this research project is elaborated in the third chapter in which process selection, mathematical model, numerical model and OpenFOAM simulations for temperature, residence time and geometry optimizations are presented while results of OpenFOAM simulations are summarized and analysed in the chapter four. In the fifth and the final chapter, conclusions derived through the analysis of results and suggestions for future works are discussed.

2. LITERATURE REVIEW

2.1 Torrefaction process

2.1.1 Introduction to biomass torrefaction

Torrefaction in other words roasting slow pyrolysis or mild pyrolysis is a relatively modern thermochemical technology where biomass is heated under atmospheric conditions in a limited oxygen environment (non-oxidizing atmosphere) at relatively low temperatures ranging in 200 – 300 ^{0}C to cause devolatilization and degradation reactions thus converting biomass into biochar which is a highly energy-dense value-added product [17]. Even though torrefaction is a recent technology in the field of thermochemical processing of biomass, there are historical records in which it is used without highlighting its name; as an example, roasting of coffee beans to enhance its flavor and brittleness. However, first reported use of torrefaction dates back to 1930 in France where wood properties were attempted to enhance for it to be used in gasifier fuel applications while first application of torrefaction in industry was reported in 1980 where biochar produced by the torrefaction of wood, was consumed as a coke substitute for silicone production. Torrefaction process gained the popularity in the recent two decades as torrefied biomass resembles properties of coal to a greater extent [18].

2.1.2 Principal and mechanism of torrefaction

Biomass is constituted with cellulose, hemicellulose, lignin and very small amount of other inorganic and organic constituents such as minerals, thus making biomass composition is mainly attributed by lignocellulose (lignin, cellulose and hemicellulose). However compositions of the main three components of biomass; i.e. cellulose, hemicellulose and lignin, depend on the biomass origin. Thermal decompositions of these three components are different due to their different molecular structural arrangements. Thermal decomposition temperatures (TDT) of cellulose, hemicellulose and lignin, are given below in the table 2-1 [19].

Table 2- 1: Thermal decomposition temperatures of cellulose, hemicellulose and lignin

Component	TDT (^{0}C)
Cellulose	315 - 400
Hemicellulose	220 -315
Lignin	160 - 900

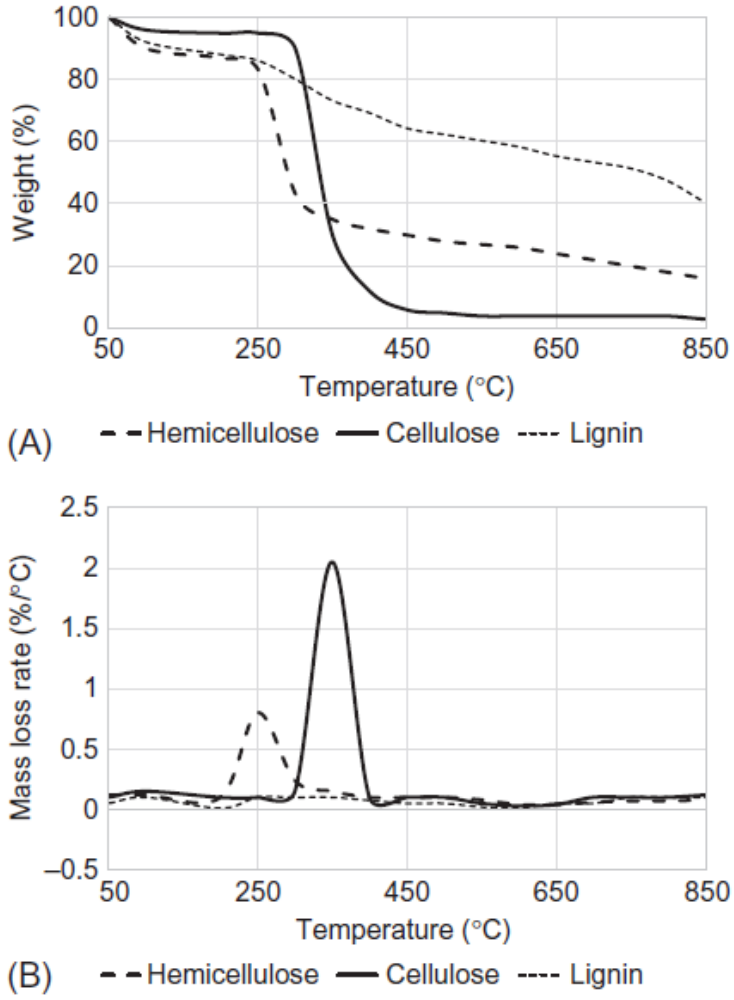

Figure 2-1: TGA and DTG curves of thermal degradation of cellulose, hemicellulose and lignin **[**18**]**

According to the thermo-gravimetric analysis curve given in the figure 2-1(A), hemicellulose and cellulose degrades rapidly respectively in 250-290 ^{0}C and 280-325 ^{0}C while lignin degrades gradually over a broad temperature range. Further derivative thermo-gravimetric analysis curve given in the figure 2-1(B) indicates that highest rate of degradation of cellulose occurs around 300 ^{0}C while that of hemicellulose occurs at 250 ^{0}C.

As a chemical interpretation for the principal of torrefaction, It can be explained that removal of oxygen and hydrogen from biomass as volatile compounds (CO_2, H_2, CH_4, H_2O and CO) with the application of heat in a comparatively slow rate such that hydrogen-carbon (H/C) and oxygen-carbon (O/C) ratios become very low thus resulting biochar in residue as shown in the van Krevelen diagram given in the figure 2-1 [20].

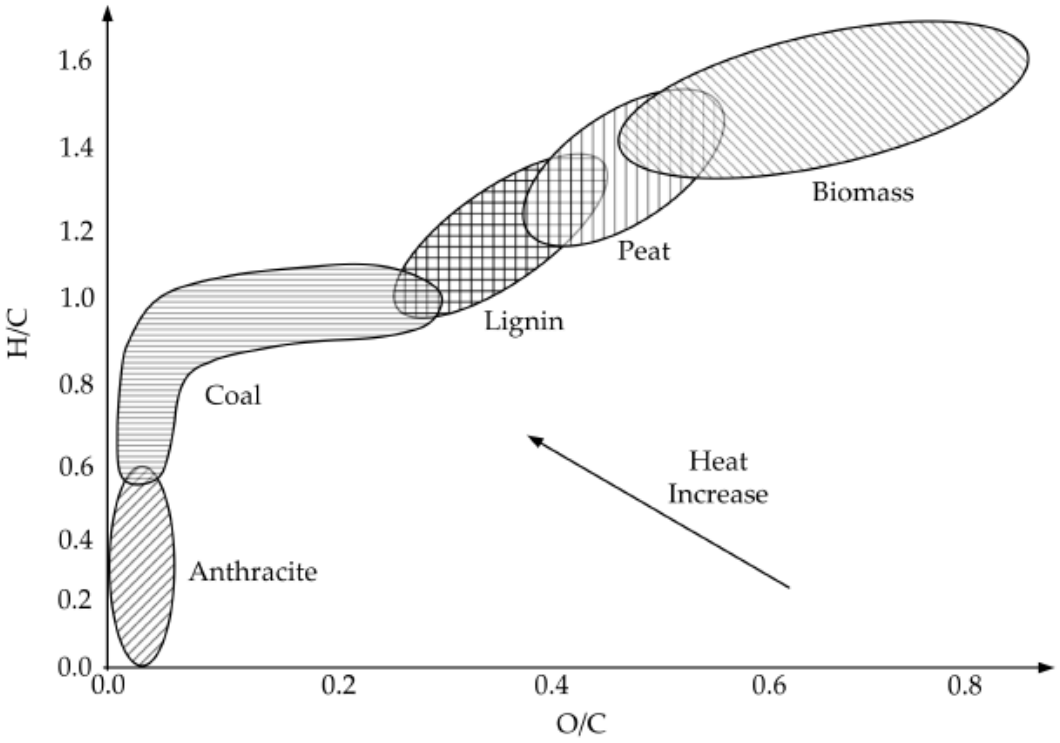

Figure 2- 2: van Krevelen diagram **[**19**]**

Torrefaction consists of five step process which occurs in different temperature and time zones as depicted in figure 2-2 given below.

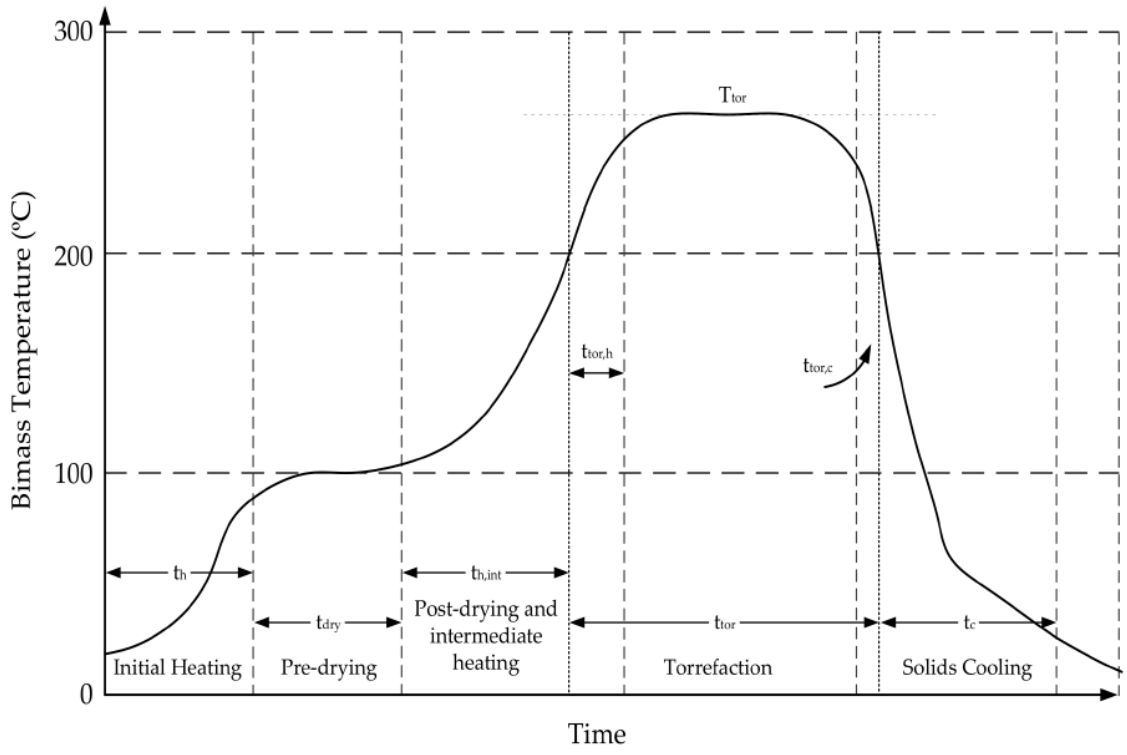

Figure 2- 3: Schematic representation of different torrefaction stages [19]

First three steps of the torrefaction process are non-reactive and in the first step, solid temperature is increased to drying temperature (100 – 120 ^{0}C). Once the solid reaches drying temperature, then it starts to evaporate unbound moisture at a stable temperature for a certain time period which is called pre-drying. As with the gradual increase of solid temperature upto 200 ^{0}C and continuation of drying, it will reach to the third stage where the remaining bound water is evaporated. In the fourth stage which is the main phase of the torrefaction process, solid temperature further marches up causing softening and depolymerization of cellulose, hemicellulose and lignin, thus initiating the thermal decomposition of main components of biomass, which is followed by heterogeneous reactions which are occurred between char and gaseous components such as CO_2, O_2

and H_2O, and gas pahse homogenous reactions. In the fifth and final step, torrefied biomass is cooled down to ambient temperature [21].

2.1.3 Effect of process parameters on torrefaction

There are numerous studies and researches conducted to analyse effect of torrefaction process parameters on overall efficiency and chemical composition & physical characteristics of biochar produced. In general, torrefaction converts biomass into less hydrophilic and high energy dense torrefied biomass which has lower O/C ratio and lower humidity [22]. In addition, torrefied biomass has more uniform properties as indicated in the following figure 2-4.

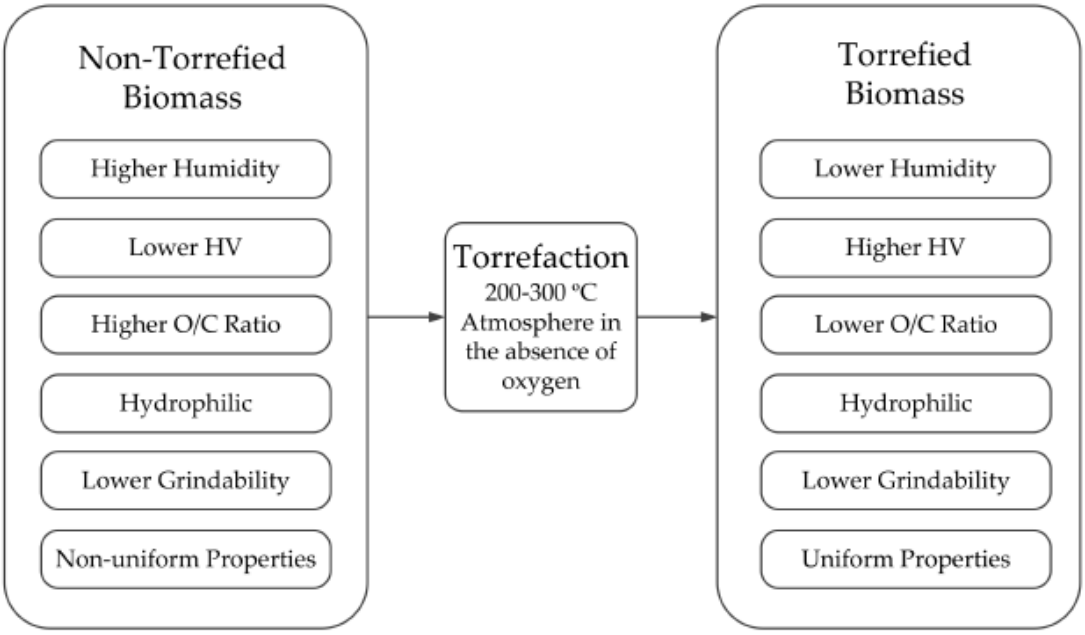

Figure 2- 4: Comparison of non-torrefied and torrefied biomass characteristics [21]

There are several parameters which affect the torrefaction process and the quality of biochar produced, from which temperature and residence time have the most prominent influence on both the productivity of overall process and the quality of biochar, while

heating rate, type of reactor & its geometry, biomass composition and process instabilities also significantly influence the torrefaction process.

- Temperature and residence time: Depending on the temperature and the time that biomass exposed to heat, degree of thermal degradation varies. Based on that, biochar yield, composition of the residue, structure & particle size and producer gas composition are determined. Temperature defines the reaction kinetics of torrefaction [22].
- Heating rate: Heating rate mainly influence the occurrence and the degree of secondary reactions which influence the final gas and solid phase compositions. In fact, when high heating rates are employed, number of secondary reactions reduces and also mass transfer between particles may weaken [23] [24].
- Type of reactor and geometry: There are different types of reactors which can be employed for torrefaction of biomass such as fixed bed reactor, continuous packed bed reactor, fluidized bed reactor, rotary drum reactor and microwave reactor [19]. Selection of particular reactor type is exclusive to the application and should be predetermined according to the heating source, process capacity, type of biomass and its composition, while geometry of the selected type of reactor should be optimized such that the process delivers required quality and yield in the most efficient way.
- Type of biomass: Type of biomass significantly affects the overall efficiency of torrefaction. For example, if green biomass or biomass having high moisture percentage is torrefied, large amount of energy is utilized in evaporation of moisture thus lowering the economic feasibility of the process tremendously. Further particle size and lignocellulose composition influence the kinetics of torrefaction reactions to a greater extent [22].
- Process instabilities: In the torrefaction process, the most influential process parameter is temperature. Quality of the biochar produced is mainly dependent of temperature profile over the residence time. Controlling of solid temperature profile is difficult due to various factors such as inertia of the process [22].

However proper control mechanism should be essential to achieve the required quality of biochar. Otherwise the temperature may go over the limits passing self-ignition temperature of torrefied biomass leading to formation of tar.

2.2 Biochar and its applications

Main product of the torrefaction of biomass is biochar while combustible gas mixture is generated as a by-product which can be combusted to generate heat. During carbonization undergoing in the torrefaction process, large part of carbon in biomass is retained while biomass is decomposed and devolatilized as volatile gases. Composition and quality of biochar varies depending on its intended application, is controlled by manipulating torrefaction process parameters accordingly. Compositions of different torrefied biomass received via proximate analysis are given below in the table 2-2.

Table 2- 2: Proximate analysis results of different torrefied biomass sources [25] [26]

Sample	Fixed carbon %	Volatile Matter %	Ash content %	Moisture %
Torrefaction of pine at 200-280 ^{0}C	27.7	71.9	0.05	0.35
Torrefaction of wood chips at 260-280 ^{0}C	36.4	62.4	1.2	4.4

Applications of biochar are diverse and hence desired characteristics of biochar differ based on the application. Some of the important applications of biochar are given below.

- As an alternative for fossil fuel to generate heat and power. Ex: boiler co-firing
- As a fertilizer and carbon sequestration agent
- Adsorption applications such as leachate treatment
- In landfill capping and phytocapping
- Remediation of contaminated soil [27]

2.3 Chemical Kinetics of Torrefaction

2.3.1 Thermal decomposition of cellulose, hemicellulose and lignin

Thermal decomposition mechanisms of cellulose, hemicellulose and lignin are different due to their structural indifferences and thus making decomposition kinetics unique to individual components. As a result, thermal decomposition of cellulose, hemicellulose and lignin should be modeled separately using specific reaction kinetics.

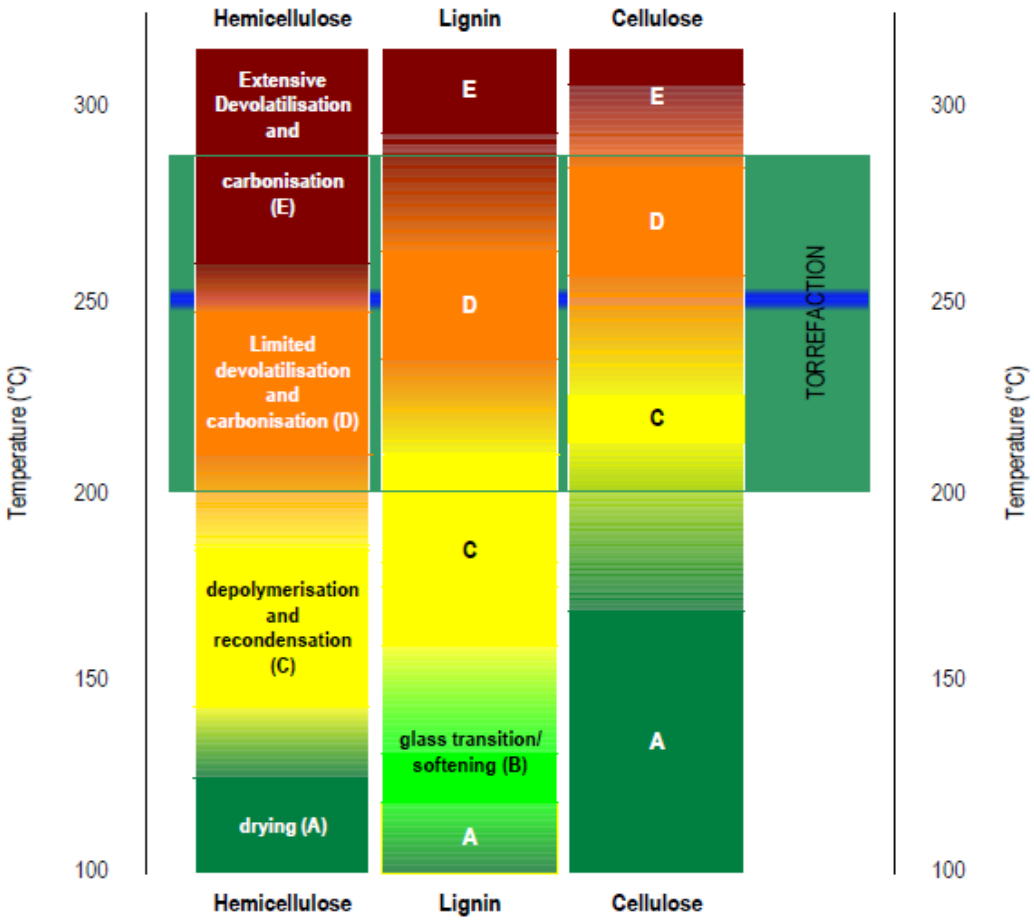

Figure 2-5: Physico-chemical phenomena during the torrefaction [21]

As shown in the figure 2-5, lignocellulose follows different reaction pathways during the torrefaction. Torrefaction reaction mechanism of both hemicellulose and cellulose follows the same order; i.e. drying > depoylmerisation and recondensation > limited devotalisation and carbonisation > extensive devoltalisation and carbonisation, even though the regime bands are distinct. On the other hand, lignin has additional identifiable reaction phase where polymers get soften before the depolymerisation [21].

First step of the torrefaction process is drying and in many research literatures the drying process is modelled by a one-step global reaction where moisture in solid-phase transfers to gas-phase [28].

$$Wet\ biomass \rightarrow Dry\ biomass + H_2O_{(g)} \quad \text{R 2: 1}$$

$$C_{2.85}H_{3.69}O.H_2O_{(s)} \rightarrow C_{2.85}H_{3.69}O_{(s)} + H_2O_{(g)} \quad \text{R 2: 2}$$

There are three types of reaction models for thermal decomposition of lignocellulose in literatures; i.e. one step global reaction model, single-stage multi reaction model and multi-stage semi global model [29]. In this research, one step global reaction model is employed where lignocellulose decomposes into char, ash and volatile gases as given by the following equations [30].

Decomposition equations of cellulose, hemicellulose and lignin;

$$Cellulose \rightarrow a_1\,C + b_1\,CO + c_1\,CO_2 + d_1\,H_2 + e_1\,CH_4 + f_1\,Ash \quad \text{R 2: 3}$$

$$Hemicellulose \rightarrow a_2\,C + b_2\,CO + c_2\,CO_2 + d_2\,H_2 + e_2\,CH_4 + f_2\,Ash \quad \text{R 2: 4}$$

$$Lignin \rightarrow a_3\,C + b_3\,CO + c_3\,CO_2 + d_3\,H_2 + e_3\,CH_4 + f_3\,Ash \quad \text{R 2: 5}$$

Stoichiometric coefficients of above equations are determined experimentally where coefficients of char and ash are determined by proximate analysis and coefficients of gaseous products are calculated according to the following equation.

$$\gamma_i = \beta_{ji} \times VF_i \quad for\ i = 1,2,3 \quad j = CO, CO_2, H_2, CH_4$$

Where,

γ_i = b_i, c_i, d_i, e_i

VF_i : Volatile fraction of i^{th} lignocellulose

β_{ji} : Distribution factor of gas j in volatile fraction of i^{th} lignocellulose

Table 2- 3: Chemical kinetic data for drying and lignocellulose decomposition reactions

Reaction	Pre-exponential factor	Activation energy	Source
R 2: 2	5.56×10^6 s^{-1}	87.9 kJ mol^{-1}	[**31**]
R 2: 3	1.379×10^{14} s^{-1}	193 kJ mol^{-1}	[**32**]
R 2: 4	2.527×10^{11} s^{-1}	147 kJ mol^{-1}	[**32**]
R 2: 5	2.202×10^{12} s^{-1}	181 kJ mol^{-1}	[**32**]

2.3.2 Solid-phase and gas-phase heterogeneous reactions

Once the lignocellulose decomposes into char and volatile gases such as CO_2, CO, H_2 and CH_4, char is reacted with gaseous products at relatively high temperatures where required activation energy for particular reaction is gained. There are three major heterogeneous reactions which occur between char, CO_2, H_2O and O_2 as given below.

$$C + CO_2 \rightarrow 2\,CO \qquad \text{R 2: 6}$$

$$C + H_2O \rightarrow CO + H_2 \qquad \text{R 2: 7}$$

$$C + \alpha\, O_2 \rightarrow 2(1-\alpha)\, CO + (2\alpha - 1)\, CO_2 \qquad \text{R 2: 8}$$

Above first two reactions are endothermic while third reaction between C and O_2 is exothermic. The parameter α given in the equation R 2:8 is dependent on the solid temperature as given by the following formula.

$$\alpha = \frac{2 + 2512e^{\frac{-6420}{T_s}}}{2(2 + 2512e^{\frac{-6420}{T_s}})}$$

Where,

T_s – Solid temperature

Table 2- 4: Kinetics of heterogeneous reactions

Reaction	Pre-exponential factor	Activation energy	Source
R 2: 6	0.652 m $s^{-1}K^{-1}$	90 kJ mol^{-1}	[**33**]
R 2: 7	3.42 m $s^{-1}K^{-1}$	129.7 kJ mol^{-1}	[**33**]
R 2: 8	3.42 m $s^{-1}K^{-1}$	129.7 kJ mol^{-1}	[**33**]

2.3.3 Gas phase homogeneous reactions

As with the generation of volatile gases, various gas phase homogeneous reactions take place and following given are the reactions which make significant impact to the torrefaction system [34].

$$CO + 0.5\ O_2 \rightarrow CO_2 \qquad \text{R 2: 9}$$

$$H_2 + 0.5\ O_2 \rightarrow H_2O \qquad \text{R 2: 10}$$

$$CH_4 + 2\ O_2 \rightarrow CO_2 + 2\ H_2O \qquad \text{R 2: 11}$$

$$CO + H_2O \rightarrow H_2 + CO_2 \qquad \text{R 2: 12}$$

All above reactions are exothermic and reaction kinetic data is given below in the table 2-5.

Table 2- 5: Reaction kinetics of gas phase homogeneous reactions

Reaction	Pre-exponential factor	Activation energy	Source
R 2: 9	2.32×10^{12} $(kmol/m^3)^{-0.75}s^{-1}$	167 kJ mol^{-1}	[**35**]
R 2: 10	1.08×10^{13} $(kmol/m^3)^{-1}s^{-1}$	125 kJ mol^{-1}	[**35**]
R 2: 11	5.16×10^{13} $(kmol/m^3)^{-0.75}s^{-1}K$	130 kJ mol^{-1}	[**35**]
R 2: 11	12.6 $(kmol/m^3)^{-1}s^{-1}$	2.78 kJ mol^{-1}	[**35**]

2.4 CFD approach to heat, mass and momentum transfer modeling

In computational fluid dynamics, mathematical model for fluid flow and heat transfer is developed using the fundamental principal of mass, momentum and energy conservation, thus deriving governing equations of fluid flow and heat transfer with use of necessary auxiliary conditions (initial and boundary conditions).

Governing equations of mass, energy and momentum transfer are based on the following conservation laws of physics [16].

- The mass of a fluid is conserved
- Newton's second law
- First law of thermodynamic

2.4.1 Navier-Stokes equations

Navier-Stokes equations are the most useful form of governing equations of fluid flow in which viscous stress model is included. For isotropic fluids in three dimensions, six components out of the nine components of linear deformation are independent. Further for Newtonian fluids, viscous stresses are proportional to the rates of linear deformations. Given below are Navier-Stokes equations for a Newtonian fluid [16].

Continuity equation;

$$\frac{\partial \rho}{\partial x} + \ div(\rho \boldsymbol{u}) \ = \ 0 \qquad \text{E 2: 1}$$

x-momentum equation;

$$\frac{\partial (\rho u)}{\partial t} + div(\rho u \boldsymbol{u}) \ = \ -\frac{\partial p}{\partial x} + \ div\big(\mu \ grad(u)\big) \ + \ S_{Mx} \qquad \text{E 2: 2}$$

y-momentum equation;

$$\frac{\partial (\rho v)}{\partial t} + div(\rho v \boldsymbol{u}) \ = \ -\frac{\partial p}{\partial y} + \ div\big(\mu \ grad(v)\big) \ + \ S_{My} \qquad \text{E 2: 3}$$

z-momentum equation;

$$\frac{\partial (\rho w)}{\partial t} + div(\rho w \boldsymbol{u}) \ = \ -\frac{\partial p}{\partial z} + \ div\big(\mu \ grad(w)\big) \ + \ S_{Mz} \qquad \text{E 2: 4}$$

Energy equation;

$$\frac{\partial (\rho i)}{\partial t} + div(\rho i \boldsymbol{u}) \ = \ -p \ div \ \boldsymbol{u} + \ div\big(k \ grad(T)\big) \ + \ \phi \ + \ S_i \qquad \text{E 2: 5}$$

Where,

ρ - Density	u - Velocity in x direction
t - Time	p - Pressure
μ - Viscosity	S_{Mx} - Source term of momentum in x direction
v - Velocity in y direction	S_{My} - Source term of momentum in y direction
w - Velocity in z direction	S_{Mz} - Source term of momentum in z direction
i - Specific internal energy	k - Thermal conductivity
ϕ - Dissipation function	S_i - Source term of specific internal energy

2.4.2 Equations of state

Equations of state are the relationships between four thermodynamic variables (internal energy, pressure, density and temperature) which are unknown in five governing equations (x-momentum, y-momentum and z-momentum equations, continuity equation and energy equation), which describe the fluid flow and heat transfer in three dimensions. Equations of state are based on the assumption that system is on thermodynamic equilibrium. State equations for pressure and specific internal energy are given by the state variables density and temperature as given below [16].

$p = p(\rho, T)$ e.g. for ideal gases; $p = \rho RT$

$i = i(\rho, T)$ e.g. for ideal gases; $i = C_v T$

2.4.3 Finite volume method

Finite difference, finite element and spectral methods are the available numerical solution techniques in CFD, and finite volume method is a special finite differencing technique which is adopted in many commercial CFD software. Finite volume method is a three step process and is represented in the figure 2-6.

Step 1: Grid generation

Grid generation is the first step of the finite volume method where application domain is divided into discrete control volumes. For a given application, common practice is to define finite number of nodal points in the space of application domain such that boundaries of control volumes are placed in between adjacent nodal points and physical boundaries are coincided with the control volume boundaries in the edge of the application domain.

Following given in the figure 2-7 is a simple schematic representation of one dimensional linear grid generation.

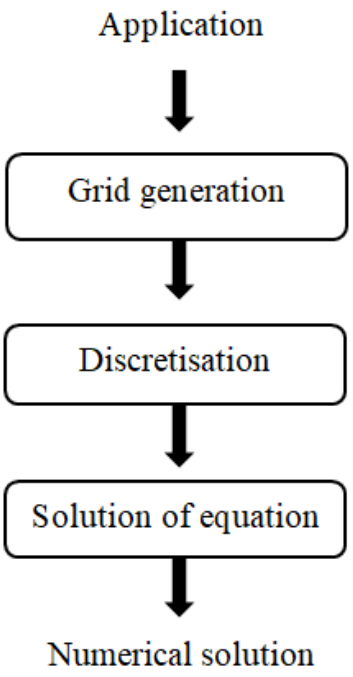

Figure 2- 6: Three steps of finite volume method

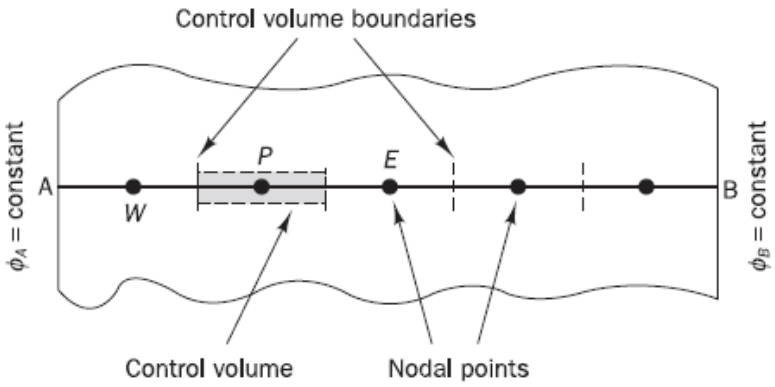

Figure 2- 7: Schematic representation of grid generation for a one dimensional case [16]

Step 2: Discretisation

Once the grid (mesh) is formed over the application domain, governing equations pertaining to the application are integrated over the control volumes and hence series of finite number of simultaneous discretised equations are generated. Then these

descretised equations are interpreted by property values of neighboring cells via numerical approximations thus generating useful form of simultaneous equations which can be computed numerically. Simplest numerical approximation to obtain interface property values and their derivatives is the linear approximation which is called central differencing [16]. Following given equations are derived via central differencing scheme for a one dimensional grid.

$$Property\ value\ at\ the\ east\ interface\ \ \emptyset_e\ =\ \frac{\emptyset_P + \emptyset_E}{2}$$

$$Property\ value\ at\ the\ west\ interface\ \ \emptyset_w\ =\ \frac{\emptyset_P + \emptyset_W}{2}$$

$$First\ derivative\ at\ the\ east\ interface\ \left(\frac{\partial \emptyset}{\partial x}\right)_e = \frac{\emptyset_E - \emptyset_P}{\delta x_{PE}}$$

$$First\ derivative\ at\ the\ west\ interface\ \left(\frac{\partial \emptyset}{\partial x}\right)_w = \frac{\emptyset_P - \emptyset_W}{\delta x_{WP}}$$

Where,

$\emptyset_P$ – Property value at node P

$\emptyset_E$ – Property value at node E

$\emptyset_W$ – Property value at node W

δx_{PE} - Length between node P and E

δx_{WP} – Length between node W and P

Depending on the application and control volume dimensions, particular approximation scheme may generate indistinguishable results from the exact solution and may not converge smoothly. However if very small control volume dimensions are possible depending on the computational capacity available, then central differencing is applicable to any application. But in practically, control volume dimensions can't be minimized freely due to the limited computational capacities. In such situations, different schemes such as upwind differencing scheme, power law scheme, ,hybrid

differencing scheme high-order differencing scheme (quadratic upwind differencing scheme QUICK and total variation diminishing schemes) are employed.

Step 3: Solution of equations

Once the discretised equations for all the nodal points in the grid are set up, these equations can be solved simultaneously by use of any suitable matrix solution technique. Following is the general form of the discretised equation for node P.

$$a_P \emptyset_P = a_W \emptyset_P + a_E \emptyset_E$$

Where; a_P, a_W and a_E are the coefficients of $\emptyset_P, \emptyset_W$ and $\emptyset_E$ respectively.

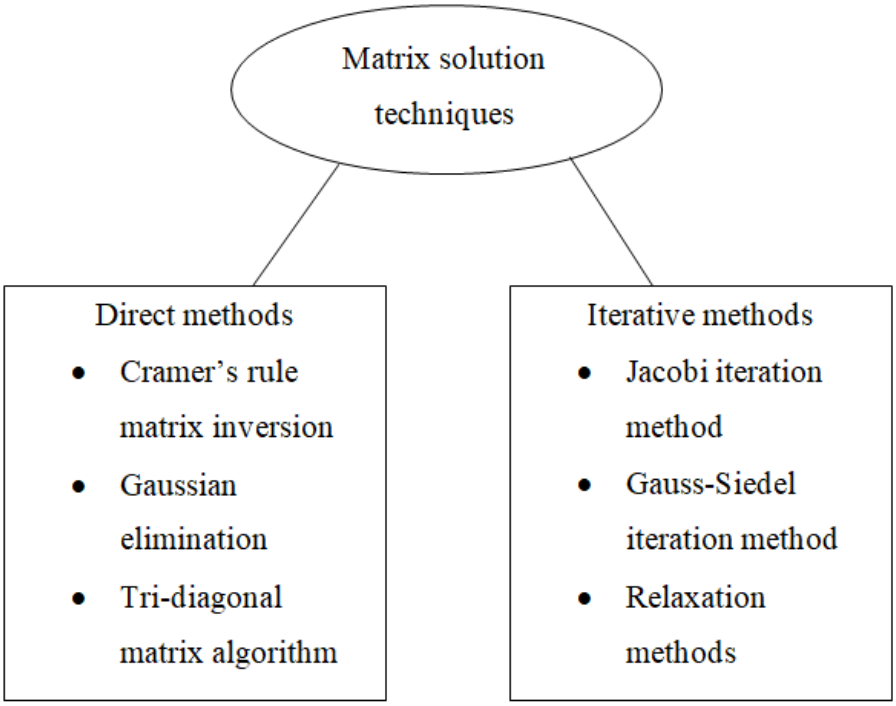

Figure 2- 8: Matrix solution techniques in CFD

Matrix solution techniques are categorized mainly into types; i.e. direct methods and iterative methods (indirect methods). Any of these solution techniques can be used in solving set of linear algebraic equations whose complexity is dependent on the

dimensionality of system, the grid and the discretization technique. However the choice of a matrix solution technique is constrained by the available computational capacities. In direct methods, more coefficients are required to be kept in the memory which in turn demands for a higher core memory while in iterative methods, relatively simple algorithms are employed where convergence is achieved after large number of repetitions thus demanding for a comparatively lesser core memory [16].

Further, there are few algorithms for pressure-velocity coupling of discretised momentum equations as given below [16].

- The SIMPLE algorithm in other words semi-implicit method for pressure-linked equations is a simple guess-and-correct procedure in which pressure is guess firstly and then discretised momentum equations are solved using the guessed pressure field which is followed by the operation of pressure correction equations.
- The SIMPLER algorithm which in short for SIMPLE revised uses discretised equations for pressure derived from the discretised continuity equations and intermediate pressure field is directly obtained without pressure corrections.
- The SIMPLEC algorithm uses special equation for velocity correction.
- The PISO algorithm is an extension of SIMPLE which is having one predictor step and two corrector steps.
- The PIMPLE algorithm is a combined algorithm of both PISO and SIMPLE.

3. STUDY METHODOLOGY

3.1 Process selection

Organic waste fraction of MSW can be processed using chemical, biochemical, thermal, thermochemical and biological technologies from which thermochemical processes are more productive for solid waste with less moisture [36]. Direct combustion, gasification, and pyrolysis are the popular thermochemical technologies but the former is a primary method and is not recommended considering the fact that it causes an uncontrolled greenhouse gas emission and doesn't yield any value addition.

In gasification, the primary objective is to convert biomass into a combustible gaseous mixture while in pyrolysis, focus is to produce value-added residue such as biochar and bio-oil. There are three types of pyrolysis; i.e. slow pyrolysis (torrefaction), fast pyrolysis and flash pyrolysis where former yields biochar while latter two types of pyrolysis mainly yield bio-oil. As torrefaction is carried out at relatively low temperatures less than 450 ^{0}C, it requires less energy for its operation compared to gasification, fast pyrolysis and flash pyrolysis [36]. Since in the present study, the objective is to produce biochar, torrefaction technology is employed.

At present, composting rate in Karadiyana composting plant is 2 Tons per day and torrefaction reactor capacity should be matched with that. As torrefaction is associated with increased residence times, in order to cater for a relatively large quantity as 2 Tons per day, batch type packed bed reactor is not feasible and thus continuous packed bed reactor is employed for this application. Hence a cylindrical reactor with varying L/D ratio (reactor length/ diameter) and a maximum capacity higher than 2 Tons per day is selected for this simulation. As with the simulation for different L/D ratios, reactor geometry can be optimized. In parallel with the optimization of reactor geometry, inlet gas temperature and residence time is subject to optimization. In order to minimize the heat loss and improve the efficiency, reactor wall is insulated.

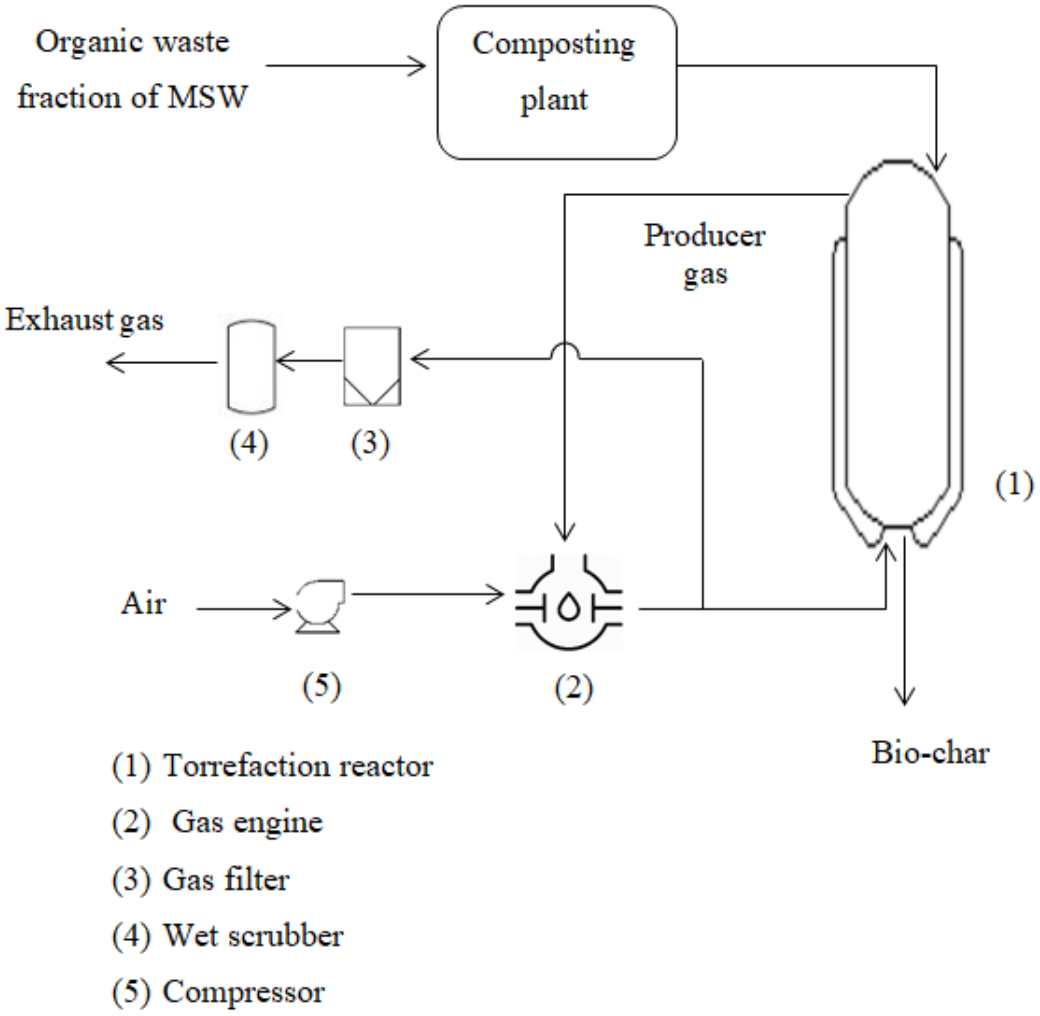

Figure 3- 1: Process flow diagram of the torrefaction process

3.2 Physical model

The torrefaction process of composted organic MSW in a cylindrical continuous packed bed reactor is a three dimensional multi-phase application which involves two phases; i.e. solid and gas phases. Composted organic MSW is continuously fed at a constant rate from the top of the reactor while hot flue gas at 200 – 350 ^{0}C is circulated from the bottom thus providing heat required for the torrefaction process. It is aimed to maintain

the solid phase temperature between 200 – 300 ^{0}C in order for the torrefaction to be occurred in the most efficient manner, which is achieved by manipulating the inlet gas temperature and velocity. Following given in the table 3-1 is proximate analysis results for composted organic MSW sample received from Karadiyana landfill site.

Table 3- 1: Proximate analysis results for dry composted organic MSW

Component	Composition (wt% dry basis)
Volatiles	76.27
Char	12.70
Ash	11.03

In the actual scenario, porous biomass particles are distributed in continuum gas-phase as depicted in the following figure 3.1. Interphase and intra-phase heat transfer occur as conduction, convection and radiation while conduction and radiation are insignificant in the heat transfer between solid and gas phases. Radiation heat which is received to solid phase from the wall of the reactor is significant as the reactor is insulated.

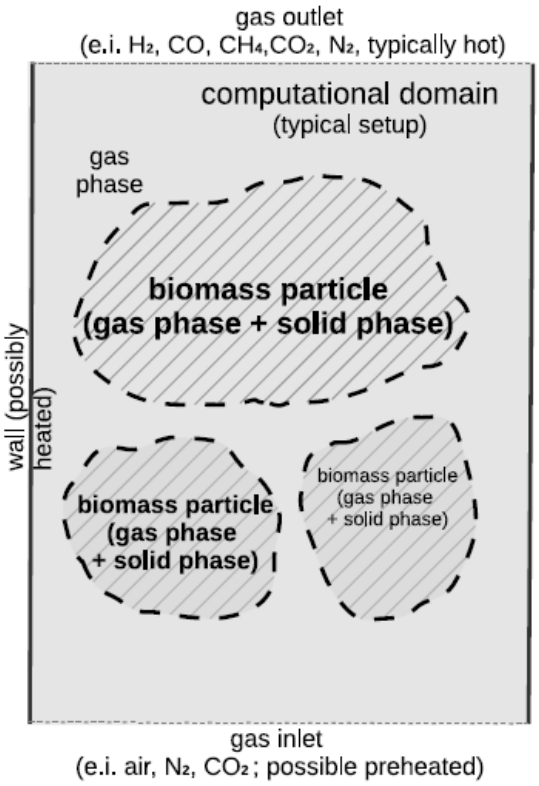

Figure 3-2: Schematic representation of porous biomass particles in an exemplary computational [40]

With the presence of gaseous components such as CO_2, CO, H_2, O_2, CH_4 and H_2O, and biochar, various homogeneous and heterogeneous reactions may occur releasing and absorbing heat from both the gas and solid phases. Therefore this torrefaction system consists of reaction sub models which impact the heat transfer, fluid flow and gas & solid phase compositions.

3.3 Mathematical Model

Physical model for the torrefaction process of organic MSW is developed into a mathematical model for a 3D transient two phase case. Eulerian-Eulerian approach is employed in the process of development of the mathematical model where several assumptions are made as given in the following section 3.2. One of the key assumptions adopted in this 3D transient, two-phase, Eulerian-Eulerian mathematical model is that both gas and solid phases are treated as continuums. Therefore motion of the solid continuum is explained by use of the continuity equation without treating solid particles separately based on the individual forces acting on them to resolve for motion parameters [13].

Effect of chemical reactions on mass and heat transfer, gas phase turbulence, and radiation heat are modeled via source terms in respective governing equations [16].

3.3.1 Governing equations

3.3.1.1 Momentum equation

Conservation equation for momentum in the gas phase is given below by the equation E 3: 2. Turbulence effect and drag force are incorporated as source terms in the momentum equation [37].

$$\frac{\partial}{\partial t}\left(\rho_g \epsilon_g \boldsymbol{U_g}\right) + \nabla.\left(\rho_g \epsilon_g \boldsymbol{U_g} \times U_g\right) - \nabla.\left(\mu \epsilon_g \nabla \boldsymbol{U_g}\right) = -\epsilon_g \nabla p + \nabla.\epsilon_g\left[\nabla \boldsymbol{U_g} + \left(\nabla U_g\right)^T - \frac{2}{3}\rho_g k \boldsymbol{I}\right] + S \qquad \text{E 3: 1}$$

$$S = 150\frac{\left(1-\epsilon_g\right)^2}{d^2{\epsilon_g}^2}U_g + 1.75\frac{\rho_g\left(1-\epsilon_g\right)\left|U_g\right|}{d^2\epsilon_g}U_g \qquad \text{E 3: 2}$$

Where,

ρ_g - Density of gas phase (kg m^{-3}) ϵ_g - Volume fraction of gas phase

U_g - Velocity of gas phase (m s^{-3}) μ - Dynamic viscosity (Pa s)

p - Pressure (Pa) k - Turbulent kinetic energy (m^2 s^{-2})

I - Second order identity tensor d - Particle size (m)

3.3.1.2 Energy equation

Conservation of energy equations for the gas and solid phases are given below in the equations E 3:3 and E 3:4. Reaction enthalpies and radiation heat are included as source terms. Optical thickness of gas phase is assumed to be very small such that gas phase absorbs negligible amount of radiation energy [13].

$$\frac{\partial}{\partial t}\left(\rho_g \epsilon_g C_{v,g} T_g\right) + \nabla.\left(\rho_g \epsilon_g C_{v,g} T_g U_g\right) - \nabla.\left(\epsilon_g k_g \nabla T_g\right) = hA\left(T_s - T_g\right) + \sum_i \Delta H_i R_{i,homo} + Q_{pyrolysis} \quad \text{E 3: 3}$$

$$\frac{\partial}{\partial t}\left(\rho_s \epsilon_s C_s T_s\right) + \nabla.\left(\rho_s \epsilon_s C_s T_s U_s\right) - \nabla.\left(\epsilon_s k_s \nabla T_s\right) = -hA\left(T_s - T_g\right) + \sum_i \Delta H_i R_{i,hetero} + Q_{drying} + Q_R \quad \text{E 3: 4}$$

Where,

T_g - Gas phase temperature (K) T_s - Solid phase temperature (K)

ρ_s - Density of solid phase (kg m^{-3}) ϵ_s - Volume fraction of solid phase

$C_{v,g}$ - Specific heat capacity of gas phase (J kg^{-1} K^{-1})

C_s - Specific heat capacity of solid phase (J kg^{-1} K^{-1})

k_g - Thermal conductivity of gas phase (W m^{-1} K^{-1})

k_s - Thermal conductivity of solid phase (W m^{-1} K^{-1})

$R_{i,hetero}$ - Rate of heterogeneous reaction i (kg m^{-3} s^{-1})

$R_{i,homo}$ - Rate of homogeneous reaction i (kg m^{-3} s^{-1})

Q_R - Radiation heat (W) h - Heat transfer coefficient (W m^{-2} K^{-1})

A - Specific surface area of bed (m^{-1}) ΔH_i - Enthalpy of the reaction i (J kg^{-1})

$Q_{pyrolysis}$ - Pyrolysis heat (W)

3.3.1.3 Species conservation equations

General species conservation equations for gas and solid phases are given in the equation E 3:5 and E 3:6 [37].

$$\frac{\partial}{\partial t}\left(\rho_g \epsilon_g Y_{g,i}\right) + \nabla.\left(\rho_g \epsilon_g Y_{g,i} U_g\right) - \nabla.\left(\epsilon_g D_{g,i} \nabla Y_{g,i}\right) = \sum_i R_{i,homo} + \sum_i R_{i,hetero} \quad \text{E 3: 5}$$

$$\frac{\partial}{\partial t}\left(\rho_s \epsilon_s Y_{s,i}\right) + \nabla.\left(\rho_s \epsilon_s Y_{s,i} U_s\right) - \nabla.\left(\epsilon_s D_{s,i} \nabla Y_{s,i}\right) = \sum_i R_{i,hetero} \quad \text{E 3: 6}$$

Where,

$Y_{g,i}$ - Mass fraction of i in the gas phase

$Y_{s,i}$ - Mass fraction of i in the solid phase

$D_{g,i}$ - Diffusion coefficient of i in the gas phase ($m^2\ s^{-1}$)

$D_{s,i}$ - Diffusion coefficient of i in the solid phase ($m^2\ s^{-1}$)

3.3.2 Reaction sub models

3.3.2.1 Drying model

As explained in the previous section 2.3.1, during the drying process, moisture embedded in wet biomass is transferred into the gas-phase as vapour or steam. In this study, drying process is modeled as a one-step global reaction according to section 2.3.1. Formula for drying rate derived based on the Arrhenius rate equation is given below for the one-step global reaction of drying **[**35**]**.

$$r_d = f_d\, e^{\left(\frac{-E_d}{R\,T_s}\right)} \epsilon_s \rho_s Y_{H_2O,s} \quad \text{E 3: 7}$$

Where,

r_d - Drying rate (kg m^{-3} s^{-1})

f_d - Pre-exponential factor (s^{-1})

E_d - Activation energy (kJ mol^{-1})

$Y_{H_2O,s}$ - Mass of fraction of moisture

3.3.2.2 Thermal decomposition model of biomass

Thermal decomposition of lignocellulose components of biomass which is also known as pyrolysis produces char, volatile gases and ash. These decomposition reactions are the core of whole torrefaction process and are modeled by using one-step global reaction schemes as explained in the section 2.3.1. Below given are the respective degradation rate equations for cellulose, hemicellulose and lignin [32].

$$r_{cel} = f_{cel}\, e^{\left(\frac{-E_{cel}}{R T_s}\right)} \epsilon_s \rho_s Y_{cel} \qquad \text{E 3: 8}$$

$$r_{hem} = f_{hem}\, e^{\left(\frac{-E_{hem}}{R T_s}\right)} \epsilon_s \rho_s Y_{hem} \qquad \text{E 3: 9}$$

$$r_{lig} = f_{lig}\, e^{\left(\frac{-E_{lig}}{R T_s}\right)} \epsilon_s \rho_s Y_{lig} \qquad \text{E 3: 10}$$

Where,

r_{cel} - Degradation rate of cellulose (kg m^{-3} s^{-1})

r_{hem} - Degradation rate of hemicellulose (kg m^{-3} s^{-1})

r_{lig} - Degradation rate of lignin (kg m^{-3} s^{-1})

f_{cel} - Pre-exponential factor of cellulose decomposition (s^{-1})

f_{hem} - Pre-exponential factor of hemicellulose decomposition (s^{-1})

f_{lig} - Pre-exponential factor of lignin decomposition (s^{-1})

E_{cel} - Activation energy of cellulose decomposition (kJ mol^{-1})

E_{hem} - Activation energy of hemicellulose decomposition (kJ mol^{-1})

E_{lig} - Activation energy of lignin decomposition (kJ mol^{-1})

Y_{cel} - Mass fraction of cellulose

Y_{hem} - Mass fraction of hemicellulose

Y_{lig} - Mass fraction of lignin

3.3.2.3 Heterogeneous reaction

Once char is formed, it undergoes combustion and gasification reactions as described in the section 2.3.2. This is a two-step process where gasifying agents first diffuse onto the surface of char particles and then undergo the heterogeneous reactions. Actual reaction rates depend not only on the kinetic rates but also on the mass transfer rates of reactant gaseous components onto the porous solid surface. In fact at elevated temperatures, rates of mass transfer are slower than the kinetics rates thus making the actual rates restricted by slow mass transfer processes [15] [13].

$$r_{k,O2} = A_c f_{O2} T_s \, e^{\left(\frac{-E_{O2}}{R\,T_s}\right)} \frac{M_c}{v_{O2} M_{O2}} \rho_{O2}$$

$$r_{k,CO2} = A_c f_{CO2} T_s \, e^{\left(\frac{-E_{CO2}}{R\,T_s}\right)} \frac{M_c}{v_{CO2} M_{CO2}} \rho_{CO2}$$

$$r_{k,H2O} = A_c f_{H2O} T_s \, e^{\left(\frac{-E_{H2O}}{R\,T_s}\right)} \frac{M_c}{v_{H2O} M_{H2O}} \rho_{H2O}$$

Where A_c specific surface area of char is given by the following formula,

$$A_c = \frac{m_{char}}{a\, m_{biomass}} A_{ss}$$

Assuming that diffusion is isotropic and diffusion perpendicular to the gas flow is negligible, mass transfer rates of O_2, CO_2 and H_2O to the surface of porous char are determined by following equations respectively [38].

$$r_{m,O2} = k_{m,O2} A_d \, (\rho_{O2} - \rho_{O2,s})$$

$$r_{m,CO2} = k_{m,CO2} A_d \, (\rho_{CO2} - \rho_{CO2,s})$$

$$r_{m,H2O} = k_{m,H2O} A_d \, (\rho_{H2O} - \rho_{H2O,s})$$

Due to the assumption of negligible diffusion normal to the gas flow, specific diffusive surface area reduces to one sixth of the total specific surface area considering a cube shaped biomass particle. The total specific area is determined based on the equation E 3:11 [13].

$$A_d = \frac{A}{6}$$

Since the prevailing temperatures in the system are high enough that kinetics rates are very high compared to mass transfer rates thus leading to the simplifying assumption that gaseous reactants take part in the reactions immediately as they reach the solid surface which make densities of gaseous reactants at the solid surface to be negligible.

Therefore $\rho_{O2,s}$, $\rho_{CO2,s}$ and $\rho_{H2O,s}$ are zero. Mass transfer coefficients of gases k_m are determined by the following formula [39].

$$Sh_i = 2 + 0.1\, Sc_i^{1/3}\, Re^{0.6}$$

$$k_{m,i} = \frac{Sh_i\, D_i}{d}$$

Where i: O_2, CO_2 and H_2O

Finally overall reaction rates are calculated by determining equivalent parallel resistances of the respective mass transfer and kinetic rates as per the following equations [39].

$$r_{O2} = \frac{r_{k,O2} \times r_{m,O2}}{r_{k,O2} + r_{m,O2}}$$

$$r_{CO2} = \frac{r_{k,CO2} \times r_{m,CO2}}{r_{k,CO2} + r_{m,CO2}}$$

$$r_{O2} = \frac{r_{k,O2} \times r_{m,O2}}{r_{k,O2} + r_{m,O2}}$$

Where,

$r_{k,O2}$, $r_{k,CO2}$ and $r_{k,H2O}$ - Kinetic reaction rate of char combustion, char CO_2 gasification and char H_2O gasification respectively (kg m^{-3} s^{-1})

f_{O2}, f_{CO2} and f_{H2O} - Pre-exponential factor of char combustion, char CO_2 gasification and char H_2O gasification respectively (m s^{-1} K^{-1})

E_{O2}, E_{CO2} and E_{H2O} - Activation energy of char combustion, char CO_2 gasification and char H_2O gasification respectively (kJ mol^{-1})

M_c, M_{O2}, M_{CO2} and M_{H2O} - Molar mass of char, O_2, CO_2 and H_2O respectively (kg/mol)

v_{O2}, v_{CO2} and v_{H2O} - Stoichiometric coefficient of O_2, CO_2 and H_2O in char combustion, char CO_2 gasification and char H_2O gasification reactions respectively

ρ_{O2}, ρ_{CO2} and ρ_{H2O} - Density of O_2, CO_2 and H_2O in the gas phase respectively (kg/m^3)

m_{char} - Mass of char per unit volume (kg m^{-3})

$m_{biomass}$ - Initial mass of biomass per unit volume (kg m^{-3})

a - Average stoichiometric coefficient of char in the degradation reactions

A_{ss} - Total specific surface area of solid phase (m^2)

$r_{m,O2}$, $r_{m,CO2}$ and $r_{m,H2O}$ - Mass transfer rate of O_2, CO_2 and H_2O (kg m^{-3} s^{-1})

$\rho_{O2,s}$, $\rho_{CO2,s}$ and $\rho_{H2O,s}$ - Density of O_2, CO_2 and H_2O in the solid surface respectively (kg/m^3)

$k_{m,O2}$, $k_{m,CO2}$ and $k_{m,H2O}$ - Mass transfer coefficient of O_2, CO_2 and H_2O respectively (m s^{-1})

Sh_i - Sherwood number of i^{th} gas

Sc_i - Schmidt number of i^{th} gas

$D_{i,g}$ - Diffusion coefficient of i^{th} gas (m^2 s^{-1})

Re - Reynolds number

3.3.2.4 Homogeneous reactions

There are four main reactions which occur in the gas phase as described in the previous section 2.3.3. Actual rate of these homogeneous reactions are limited by turbulent mixing rates where reactants are not mixed together well specially in the areas near to

the reactor wall. These reactions usually progress at kinetic rates in free board area and away from the wall where sufficient turbulent mixing is taken place. As a result, based on the limiting assumption mentioned above, actual reaction rate is determined as the minimum of the kinetic rate and the respective turbulent mixing rate [15] [35].

$$r_i = min(r_{k,i} - r_{t,i})$$

Kinetic rates for reactions R 2:9, R 2:10, R 2:11 and R 2:11 are modeled as below.

$$r_{k,2.9} = f_{2.9}\, e^{(\frac{-E_{2.9}}{R\,T_g})}\,[CO][O_2]^{0.25}[H_2O]^{0.5}$$

$$r_{k,2.10} = f_{2.10}\, e^{(\frac{-E_{2.10}}{R\,T_g})}\,[H_2][O_2]$$

$$r_{k,2.11} = f_{2.11}\, T_g^{-1} e^{(\frac{-E_{2.11}}{R\,T_g})}\,[CH_4][O_2]$$

$$r_{k,2.12} = f_{2.12}\, e^{(\frac{-E_{2.12}}{R\,T_g})}\left([CO][H_2O] - \frac{[CO_2][H_2]}{0.0265\, e^{(\frac{3968}{T_g})}}\right)[CH_4][O_2]$$

Based on the eddy dissipation model, turbulent mixing rates are modeled as given below [15].

$$r_{t,i} = 4\rho_g \frac{\in}{k} min\left(\frac{Y_j}{v_j M_j} - \frac{Y_k}{v_k M_k}\right)$$

Where,

$r_{k,i}$ - Kinetic reaction rate of ith equation (kmol m^{-3} s^{-1})

f_i - Pre-exponential factor of ith equation

E_i - Activation energy of ith equation (kJ mol^{-1})

$[H_2], [O_2], [CO], [H_2O], [CO_2]$and $[CH_4]$ - Concentration of H_2, O_2, CO, H_2O, CO_2 and CH_4 in the gas phase (kmol m^{-3})

$r_{t,i}$ - Turbulent mixing limited reaction rate (kmol m^{-3} s^{-1})

ρ_g - Density of gas (kg m^{-3})

k - Turbulent kinetic energy (m^2 s^{-2})

$\in$ - Turbulent dissipation rate (m^2 s^{-3})

Y_j and Y_k - Mass fraction of reactants of reaction i

v_j and v_k - Stoichiometric metric coefficient of reactants of reaction i

M_j and M_k - Molar mass of reactants of reaction i (kg $kmol^{-1}$)

3.3.3 Heat transfer sub models

In the governing equations for energy, terms in the right hand side represent energy generation due to the sources. All of convective heat transfer, radiation and reactions heats, drying and pyrolysis heats are included as source terms in the governing equations and respective sub models are developed accordingly as following sections elaborate.

3.3.3.1 Inter-phase heat transfer model

Inter-phase heat transfer between the gas and solid phases is occurred as a result of convective heat transfer driven by the temperature gradient exists between the two phases and is modeled by use of an overall heat transfer coefficient based on the assumption that mean heat transfer coefficient exists such that overall effect of convection for a very small part of solid continuum negligibly differs from the actual integration of interphase convection heat of infinitesimal volumes [13] [15].

$$Q_{sg} = hA\left(T_s - T_g\right) \quad \text{E 3: 12}$$

$$A = \frac{6\,\epsilon_s}{d} \quad \text{E 3: 11}$$

$$h = \frac{k_g \epsilon_g Nu}{d} \quad \text{E 3: 13}$$

$$Nu = \left(7 - 10\epsilon_g + 5\epsilon_g^2\right)\left(1 + 0.7Re^{0.2}Pr^{0.33}\right) + \left(1.33 - 2.4\epsilon_g + 1.2\epsilon_g^2\right)Re^{0.2}Pr^{0.33} \quad \text{E 3: 14}$$

Where,

Q_{sg} - Interphase convective heat transfer rate (W)

A - Specific surface area of solid (m^{-1})

Nu - Nusselt number

Re - Reynolds' number

Pr - Prandtl number

3.3.3.2 Radiation model

Radiation is a very significant means of transporting heat within the reaction vessel as the vessel is thermally insulated and the solid temperature is elevated to temperatures as high as 600 ^{0}C. For this case, it is assumed that solid phase both emits and absorbs radiation energy while gas phase doesn't take part in absorbing or emitting radiation energy. Following assumptions are made in the process of development of the radiation model [35] [13].

- Solid phase is dispersed medium of solid particles which absorbs, emits and scatters radiation energy.
- Reactor wall is an emissive plate of radiation.
- Gas phase is optically thin and doesn't not absorb and emit radiation.

$$\nabla.(\Gamma\,\nabla G) + 4\left(an^2\sigma T_g^4 + E_p\right) - \left(a + a_p\right)G = 0 \qquad \text{E 3: 15}$$

Where Γ and E_p are given by,

$$\Gamma = \frac{1}{3(a + a_p + \sigma_p)} \qquad \text{E 3: 16}$$

$$E_p = \varepsilon\, A_r\, T_s^4 \qquad \text{E 3: 17}$$

Where,

G - Incident intensity (W/m^2)

a - Absorption coefficient of gas phase (m^{-1})

a_p - Absorption coefficient of solid phase (m^{-1})

n - Refractive index of gas phase

σ - Stefan constant ($W\ m^{-2}\ K^{-4}$)

E_p - Equivalent emission of particles

A_r - Specific surface area available for radiation (m^{-1})

ε - Emissivity of solid particles

Since gas phase is optically thin, a = 0 and n = 0. Therefore the above governing equation E 3: 11 simplifies into the following equation E 3: 14.

$$\nabla.(\Gamma\ \nabla G) + 4\ E_p - a_p G\ =\ 0 \qquad \text{E 3: 18}$$

Radiation heat flux (q_r) is given by the below equation E 3: 15.

$$q_r\ =\ -\Gamma\ \nabla G \qquad \text{E 3: 19}$$

Further radiation source term in the energy equation E 3: 4

$$Q_R\ =\ -\nabla q_r \qquad \text{E 3: 20}$$

$$Q_R\ =\ a_p G\ -\ 4\ E_p \qquad \text{E 3: 21}$$

3.3.3.3 Drying heat

As with the moisture bound to biomass is vaporised and released into the gas phase, energy is carried away from the solid phase to the gas phase. In the present study, it is assumed that total evaporation energy is transferred to the gas phase without any loses. Following equation E 3: 22 is employed to calculate the heat of evaporation.

For fiber saturation point < $Y_{moisture}$;

$$H_{evp}\ =\ 3179 - 2.5\ T_s\ + 1176.2\ e^{(-15\ Y_{moisture})} \qquad \text{E 3: 22}$$

$$Drying\ heat\ =\ r_d\ \times\ H_{evp} \qquad \text{E 3: 23}$$

Where,

H_{evp} - Heat of evaporation (kJ kg^{-1} m^{-3})

$Y_{moisture}$ - Mass fraction of moisture

r_d - Drying rate (kg m^{-3} s^{-1})

3.3.3.4 Torrefaction heat

Torrefaction heat or in other words energy liberated during the reactions of decomposition of cellulose, hemicellulose and lignin is assumed to be transferred into the gas phase as hot volatile gases liberate from the reactions. Energy carried away with the hot volatile gases into the gas phase is modelled as below [40].

$$E_{tor} = R_{biomass} C_{v,g} (T_s - T_g) \quad \text{E 3: 24}$$

$$R_{biomass} = r_{cel} + r_{hem} + r_{lig} \quad \text{E 3: 25}$$

Where,

E_{tor} - Torrefaction heat (kJ m^{-3})

$C_{v,g}$ - Specific heat of gas (kJ K^{-1} kg^{-1})

$R_{biomass}$ - Decomposition rate of biomass (kg m^{-3} s^{-1})

3.3.3.5 Chemical reactions

Energies released or absorbed due to exothermic and endothermic reactions occur in the system are determined based on the respective reaction enthalpies and they are modelled by the following general equation.

$$E_{Ri} = r_i \times H_i \quad \text{E 3: 26}$$

Where,

E_{Ri} - Energy released or absorbed due to the reaction i (kJ m^{-3})

r_i - Rate of the reaction i (kmol m^{-3} s^{-1})

H_i - Enthalpy of the reaction I (kJ mol^{-1})

3.3.4 Modeling of physical properties

Specific heat capacity and thermal conductivity of gas and solid phases are determined based on the following equations E 3:27, E 3:28, E 3:29 and E 3:30 sourced from the literature [31] [39] [13].

$$k_g = 4.8 \times 10^{-4}\, T_g^{0.717} \qquad \text{E 3: 27}$$

$$k_s = 0.8\, k_g + 0.5\, Re\, Pr\, k_g \qquad \text{E 3: 28}$$

$$C_s = 420 + 2.09\, T_s + 6.85 \times 10^{-4}\, T_s^2 \qquad \text{E 3: 29}$$

$$C_g = 990 + 0.122\, T_g - 5680 \times 10^{3}\, T_g^{-2} \qquad \text{E 3: 30}$$

Volume fraction of solid phase, volume fraction of gas phase and kinetic viscosity of gas phase are given by the following equation

$$\epsilon_s = \frac{m_{biomass}}{\rho_{biomass}} + \frac{m_{char}}{\rho_{char}} + \frac{m_{ash}}{\rho_{ash}} \qquad \text{E 3: 31}$$

$$\epsilon_g = 1 - \epsilon_s \qquad \text{E 3: 32}$$

$$\eta = 1.98 \times 10^{-5}\, \frac{T_g}{300\, \rho_g} \qquad \text{E 3: 33}$$

Binary diffusion coefficients of individual gases in gas phase is assumed to be similar as their diffusion coefficients in air and calculated based on the following equation E 3: 34.

$$D_{i,g} = 0.0018583 \sqrt{T_g^3 \left(\frac{1}{M_i} + \frac{1}{M_{air}}\right)} \frac{1}{p\sigma_{i,air}^2 \Omega_{i,g}} \qquad \text{E 3: 34}$$

Where diffusion collision integral of ith gas in air $\Omega_{i,g}$ is given by the following equation E 3: 35

$$\Omega_{i,g} = \left(44.54\, (k_{i,g} T_g)^{-4.909} + 1.911\, (k_{i,g} T_g)^{-1.575}\right)^{0.1} \qquad \text{E 3: 35}$$

$\sigma_{i,air}$ – Average collision diameter (A)

Dimensionless numbers Re, Pr and Sc are given by the below equations E 3:36, E 3:37 and E 3:38.

$$Re = \frac{d\,|U|}{\eta} \qquad \text{E 3: 36}$$

$$\Pr = \frac{c_g \eta \rho_g}{k_g} \qquad \text{E 3: 37}$$

$$Sc_i = \frac{\eta}{D_{i,g}} \qquad \text{E 3: 38}$$

3.3.5 Assumptions

- Gas and solid phases are assumed to be continuums
- Optical thickness of gas phase is insignificant such that gas phase doesn't take part in absorbing, emitting or scattering radiation energy
- Solid phase is considered to be a medium which absorbs, scatters and emits radiation energy
- Effect of reducing biomass particle size during the process is insignificant
- Solid velocity is assumed to be constant throughout the process and opposite gas flow has negligible effect on the solid velocity
- Solid only flows in the axial direction (Z direction)
- Reactor wall is assumed to be perfectly insulated that heat loss to outside through the wall is zero
- Generated steam and volatile gases increased the energy of gas phase according to the equations 3-23 and 3-24 respectively
- The reactor wall is considered to be a radiation energy emitting media

- There exist only the three major heterogeneous reactions as given in the section 2.3.2 which have significant impacts on the system
- Composted organic MSW (biomass) is only consisted of moisture and main lignocellulose components i.e. cellulose, hemicellulose and lignin, and presence of other components is assumed to be negligible
- It is assumed that decomposition reactions of cellulose, hemicellulose and lignin are one-step global reactions
- Drying reaction is assumed to be a one-step global reaction and both free and bound moisture are evaporated in the similar manner
- There exist only four major homogeneous reactions as given in the section 2.3.3, which affect the system significantly and those four reactions are assumed to be one-step global reactions
- In the calculation of gas species diffusion into the solid surface, a solid particle is considered as cubic in shape and thus previous assumption reduces the specific diffusive surface area to one sixth of the total specific surface area.
- Gas species which undergo heterogeneous reactions are assumed to be taken part in the conversion as immediately as they reach to the solid surface and hence densities of those gases in the vicinity of the solid surface are assumed to be negligible.

3.4 OpenFOAM simulation

The mathematical model developed in the previous section for the torrefaction of composted organic waste is then transformed into a numerical model by using open source CFD software OpenFOAM, version 7.0. Mathematical expressions in the model are coded into the numerical model by C++ language in which equations are discretised and hence solved numerically using finite volume method. Inbuilt libraries of OpenFOAM are employed in the code where necessary. As the first step of the development of numerical model, solution algorithm is built and is presented in the figure 3-3. Simulations are processed in a 64-core high performance computer (64 Gb RAM and 2.2 GHz processor speed) in parallel computing mode.

3.4.1 Mesh generation

Since a 3D solution domain is required for this application, a 3D grid is developed for the numerical model by using the OpenFOAM mesh generation package BlockMesh. The grid is built integrating five blocks which are hexahedrons with curved edges (four of them are similar) as depicted in the figure 3-4. Dimension of a general cell is also given in the same figure 3-4. General cell dimensions are set as Δx = 0.0218 m and Δy = 0.0142 with an aspect ratio of 3:2.

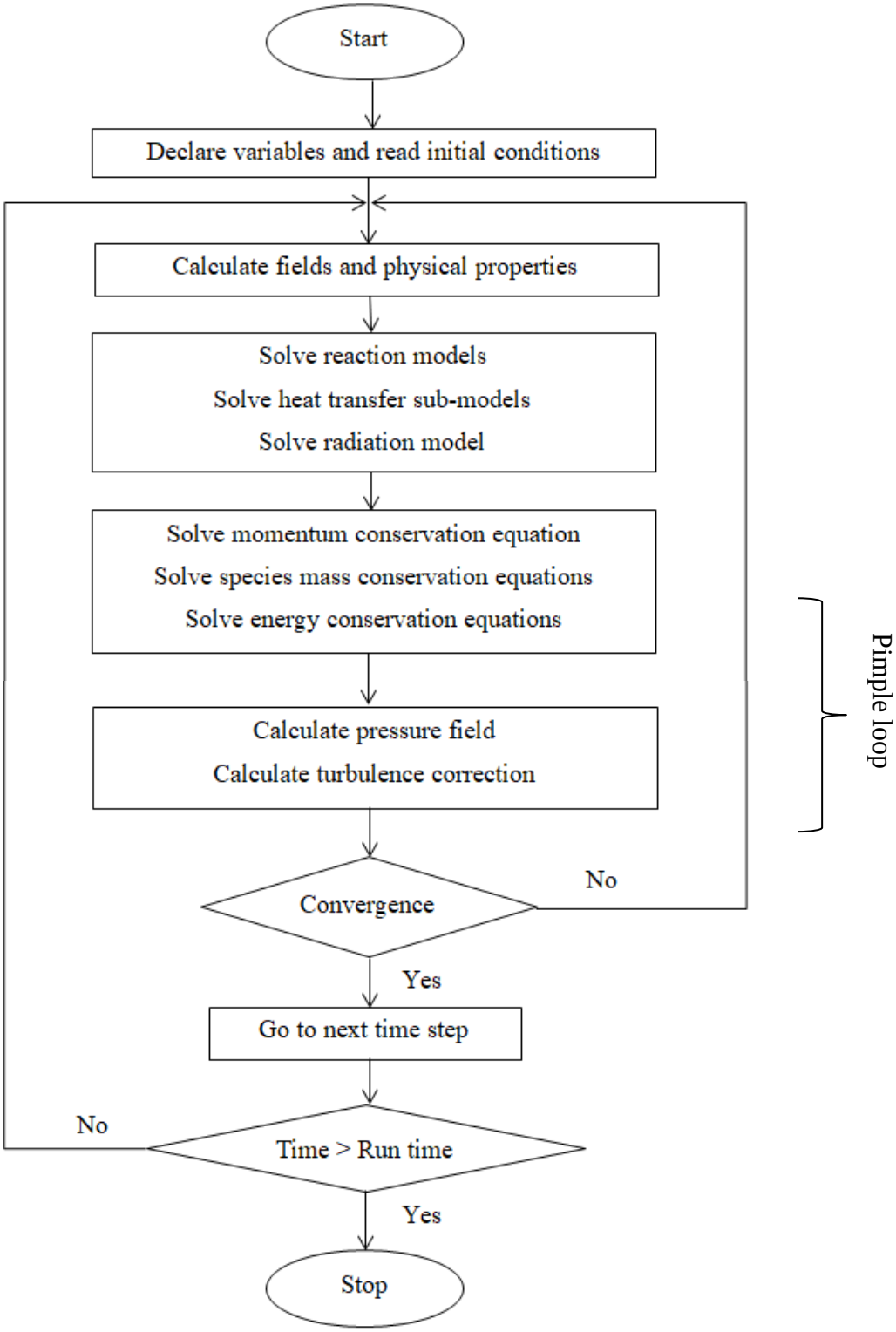

Figure 3-3: Schematic representation of solution algorithm

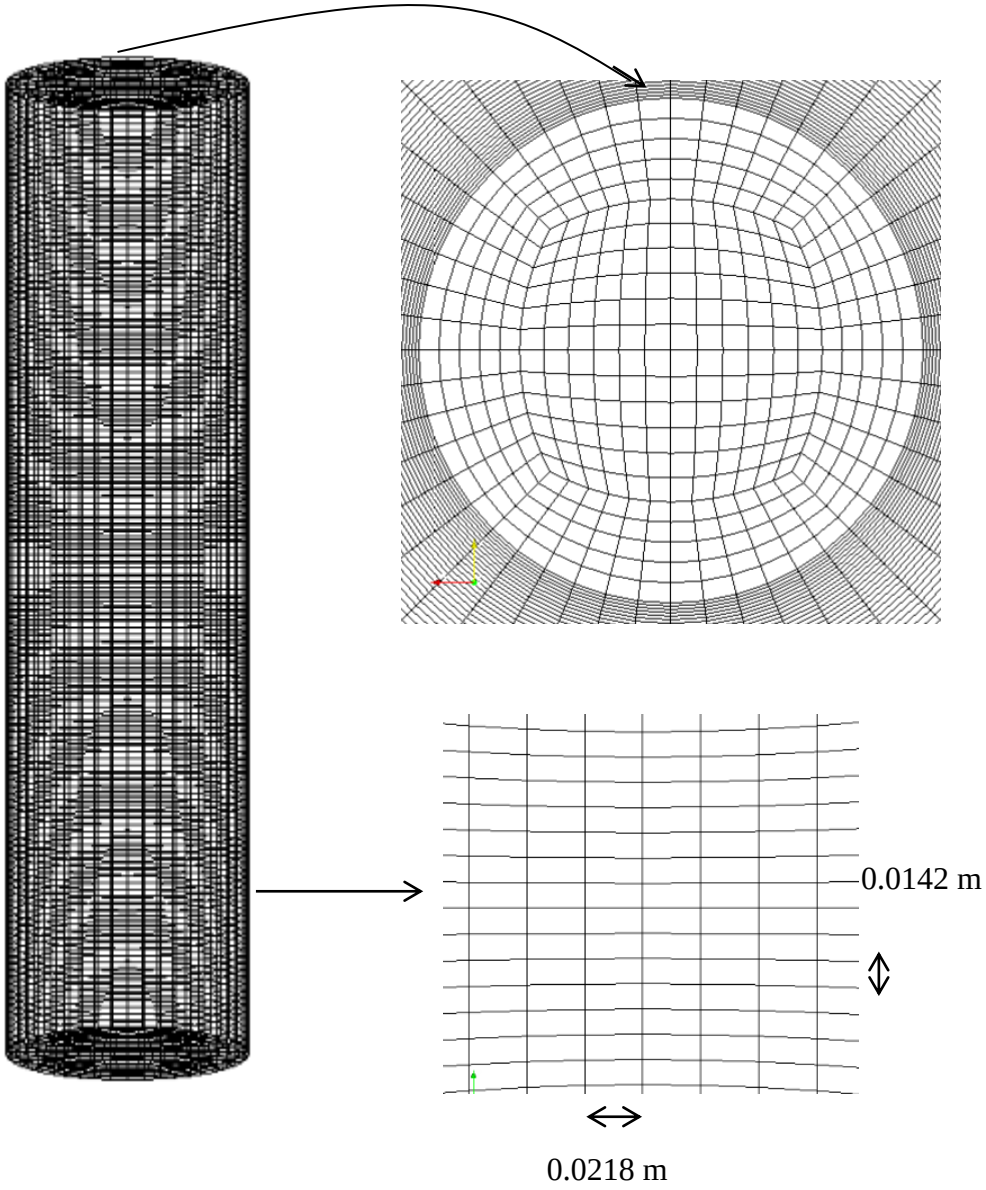

Figure 3- 4: 3D grid developed for the solution domain

3.4.2 OpenFOAM simulation Parameters

Following discretization schemes given in the table 3-1 are employed in the OpenFOAM simulation. Further the solvers used in matrix calculations are given in the table 3-2.

Table 3- 2: Discretisation schemes

Term	Scheme
Time derivatives $\frac{\partial}{\partial t}$	Euler
∇p Other grad terms ∇	Gauss linear cellLimited Gauss linear 1
$\nabla.\left(\rho_g \epsilon_g \mathbf{U_g} \times U_g\right)$ $\nabla.\left(\rho_g \epsilon_g C_{v,g} T_g U_g\right), \nabla.\left(\rho_s \epsilon_s C_s T_s U_s\right)$ $\nabla.\left(\rho_g \epsilon_g Y_{g,i} U_g\right)$ $\nabla.\left(\rho_s \epsilon_s Y_{s,i} U_s\right)$ Other divergent terms	Gauss limitedLinearV 1 Gauss limitedLinear 1 Gauss limitedLinear01 1 Gauss linear Gauss linear
Laplacian terms	Gauss linear limited corrected 0.5
Interpolation	linear

Table 3- 3: Matrix solvers

Variable	Solver	Tolerance
p, Y_s, k, epsilon	PBiCG - Preconditioned (bi-) conjugate gradient	1×10^{-6}
U, T_g, T_s, Y_s	PBiCGStab – Stabilised preconditioned (bi-) conjugate gradient	1×10^{-6}
G	PCG – Preconditioned conjugate gradient	1×10^{-6}

Given below are the control parameters of OpenFOAM simulations.

Table 3- 4: Control parameters of the simulations

Parameter	Value
Simulation type	Laminar
Delta t	1×10^{-5} s
Maximum number of iteration	1000
Maximum courant number	0.07
Write precision	10
Time precision	10

3.4.3 Initial and boundary conditions

In this application as explained in the section 3.1, composted organic MSW is torrefied in a cylindrical reactor whose wall is insulated. Hot gas from a combustor is supplied from the bottom of the reactor as the inlet gas stream which provides the required energy for the torrefaction process while composted biomass is fed from the top of the reactor continuously. There are three boundary walls i.e; wall, top and bottom as depicted in the figure 3-4. The initial values and boundary conditions associated with this application are summarized in the following table 3-4.

Table 3- 5: Initial and boundary condition of the model

Parameter	Initial value	Boundary conditions
T_g	Internal filed: 300K	Wall: Zero gradient Top: Zero gradient Bottom: Fixed value (473, 523, 573, 623K)
T_s	Internal filed: 300K	Wall: Zero gradient Top: Fixed value (300K) Bottom: Zero gradient
U	Internal field: [0 0 0] m/s	Wall: non slip Top: Zero gradient Bottom: Fixed value [0 0 0.08] m/s
$m_{cellulose}$ $m_{hemicellulose}$ m_{lignin} $m_{moisture}$	Internal field: Uniform $m_{cellulose}$: 187.54 kg/m^3 $m_{hemicellulose}$: 76.19 kg/m^3 m_{lignin} : 29.30 kg/m^3 $m_{moisture}$: 67.50 kg/m^3	Wall: Zero gradient Top: Fixed value $m_{cellulose}$: 187.54 kg/m3 $m_{hemicellulose}$: 76.19 kg/m3 m_{lignin} : 29.30 kg/m3 $m_{moisture}$: 67.50 kg/m3 Bottom: Zero gradient
m_{char} m_{ash}	Internal field: Zero/Uniform	Wall: Zero gradient Top: Fixed value Bottom: Zero gradient
$m_{CO2,g}$ $m_{CO,g}$ $m_{O2,g}$ $m_{H2,g}$ $m_{H2O,g}$ $m_{N2,g}$	Internal field: Uniform	Wall: Zero gradient Top: Zero gradient Bottom: Fixed value (kg/m^3) $m_{CO2,g}$: 0.245 $m_{CO,g}$: 0.001 $m_{O2,g}$: 0.0375 $m_{H2,g}$: 0 $m_{H2O,g}$: 0.212 $m_{N2,g}$: 0.747

3.4.4 Optimization of residence time and temperature

In the torrefaction system of the present study, main independent variables which can be effectively controlled are inlet gas temperature, inlet gas velocity and solid velocity. In fact the inlet gas temperature & velocity and the solid velocity decide the solid temperature profile and its dynamics over the time span of interest; i.e. residence time, while on the other hand residence time is solely dependent on the solid velocity neglecting the effect of resistance imposed by the opposite gas flow. Further the effects of temperature and residence time on the efficiency of overall torrefaction process are very much difficult to analyse separately due to their coupling effect and hence the residence time and the temperature are optimized together in parallel.

3.4.5 Optimization of reactor geometry

Once the optimum residence time and temperature combination is determined, reactor geometry is optimized for those values of residence time and inlet gas temperature. Geometrical optimization of the reactor is carried out by running simulations for varying L/D ratio. In the present study, length of the reactor 2m is kept constant while diameter of the reactor is varied so that simulations are carried out for different L/D ratios.

4. RESULTS & DISCUSSION

4.1 Optimization of temperature and residence time

In order for the optimization of temperature and residence time, simulations were run for different inlet gas temperature and residence time combinations. Simulations were carried out at four different inlet gas temperatures 473K, 523K, 573K and 623K and further for each gas inlet temperature value, simulations were repeated for five different residence times i.e. 8000s, 10000s, 12000s, 13000s and 14000s. Altogether 20 number of simulations was carried out one by one in a 64-core high performance computer in parallel mode. Numerical results obtained from the OpenFOAM simulation were graphically interpreted and analysed using paraFOAM which is the main post-processing tool provided with OpenFOAM. paraFOAM is an open-source graphical user interface for visualization of numerical results. Following given in table 4-1, table 4-2, table 4-3 and table 4-4 are profiles of solid temperature (K), char formation (kg/m^3), biomass concentration (kg/m^3) and ash generation (kg/m^3) respectively obtained from paraFOAM.

Table 4- 1 Solid temperature (Ts) profiles

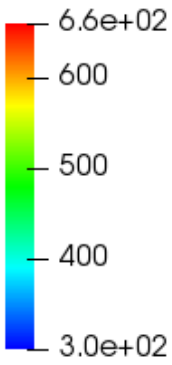

	473 K	523 K	573 K	623 K
8000 s				

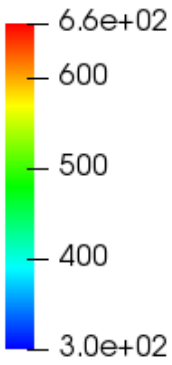

	473 K	523 K	573 K	623 K
10000 s				

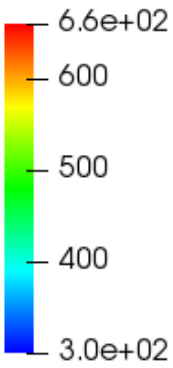

	473 K	523 K	573 K	623 K
12000 s				

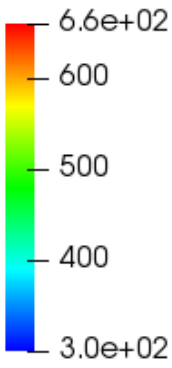

	473 K	523 K	573 K	623 K
13000 s				

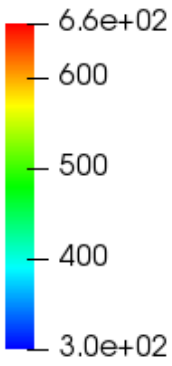

	473 K	523 K	573 K	623 K
14000 s				

Table 4- 2: Char formation (kg/m^3)

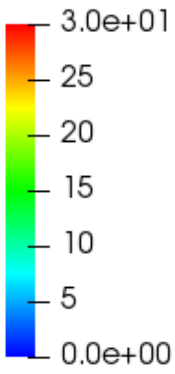

	473 K	523 K	573 K	623 K
8000 s				

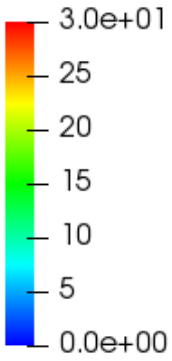

	473 K	523 K	573 K	623 K
10000 s				

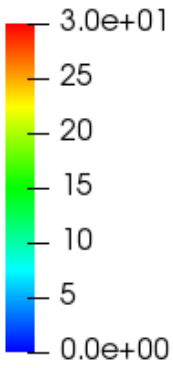

	473 K	523 K	573 K	623 K
12000 s				

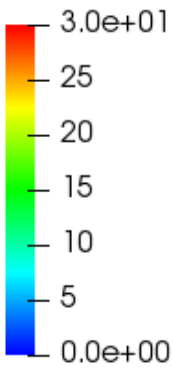

	473 K	523 K	573 K	623 K
13000 s				

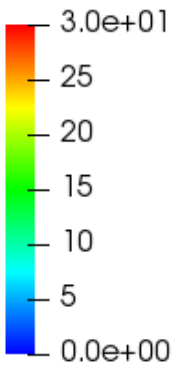

	473 K	523 K	573 K	623 K
14000 s				

Table 4- 3: Lignocellulose per unit volume (kg/m^3)

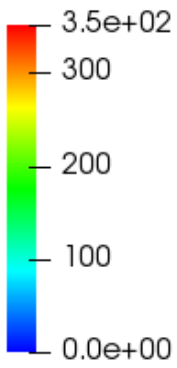

	473 K	523 K	573 K	623 K
8000 s				

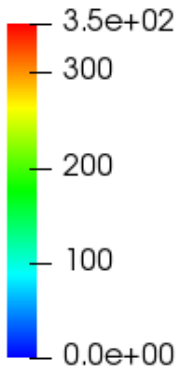

	473 K	523 K	573 K	623 K
10000 s				

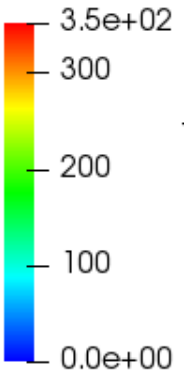

	473 K	523 K	573 K	623 K
12000 s				

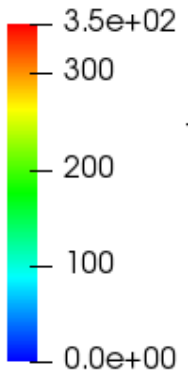

	473 K	523 K	573 K	623 K
13000 s				

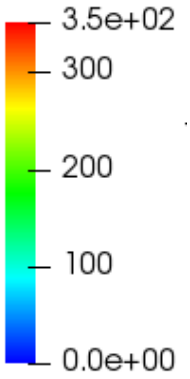

	473 K	523 K	573 K	623 K
14000 s				

Table 4- 4: Ash generation (kg/m^3)

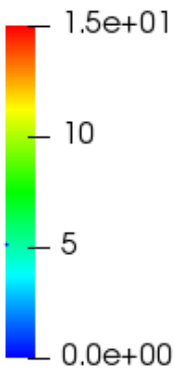

	473 K	523 K	573 K	623 K
8000 s				

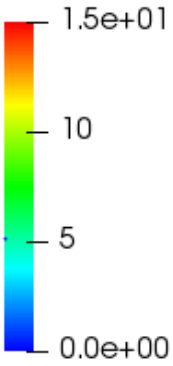

	473 K	523 K	573 K	623 K
10000 s				

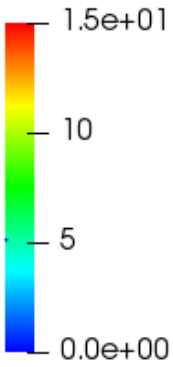

	473 K	523 K	573 K	623 K
12000 s				

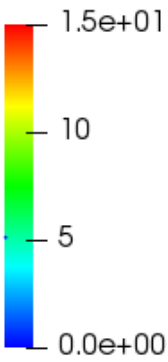

	473 K	523 K	573 K	623 K
13000 s				

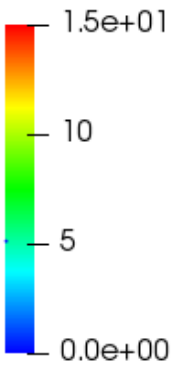

	473 K	523 K	573 K	623 K
14000 s				

4.2 Analysis of results

Based on the literature discussed in the section 2.3.1, reactions zones in the solution domain were identified with respect to the lignocellulose composition as depicted in the figure 4-1. Basically there are four zones where drying is occurred in the first zone and then softening and depolymerization of lignocellulose undergo in the second zone. Third and fourth zones together are identified as the torrefaction zone where the carbonization is progressed. Further limited devolatilization and carbonization undergo in the third zone while it is extensive occured in the fourth zone.

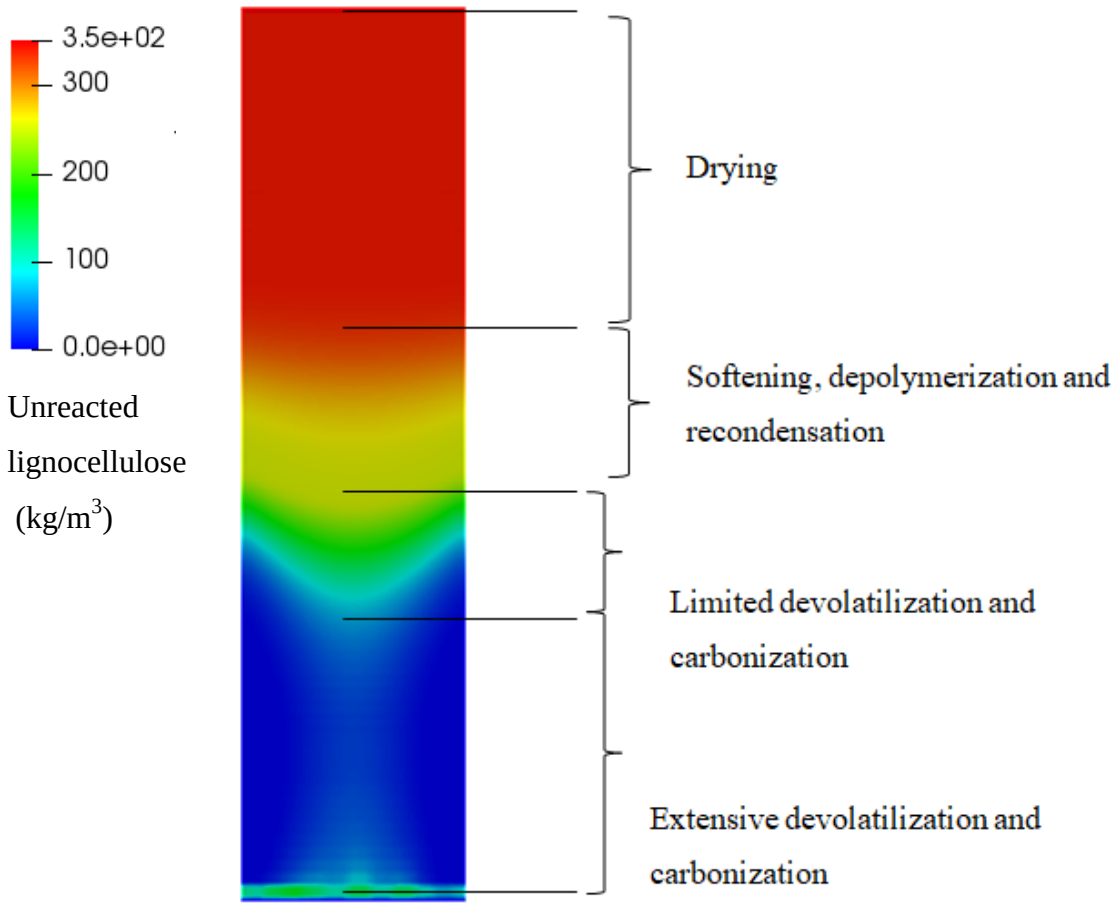

Figure 4- 1: Reaction zones in the solution domain

In the bottom part of the reactor, there exists a high temperature zone in the neighboring region of wall and it gets broaden with the time which can be clearly observed in solid temperature profile given in the table 4-1. This is a result of gas velocity and heat transfer. When the gas velocity is low, gas phase to solid phase heat transfer increases. Following figure 4-10 is a gas velocity profile taken at 14000s for 573K inlet gas temperature and there it can be noticed that corresponding low gas velocity region has been created. In this region, extensive carbonization is occurred as in the figure 4-9.

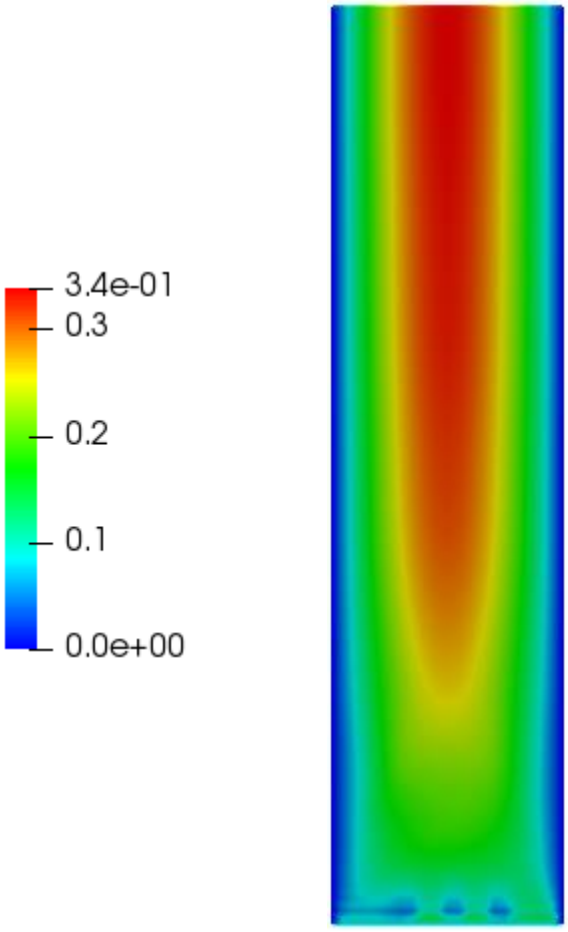

Figure 4- 2: Gas velocity profile at 14000s for 573K inlet gas temperature

Table 4- 5: Char yield percentage in outlet for different temperatures and residence times

Temperature / R. Time	473K	523K	573K	623K
8000s	0.5	1.0	1.9	2.4
10000s	2.1	3.4	4.1	4.7
12000s	9.0	11.8	18.8	22.8
13000s	42.3	48.1	55.7	58.1
14000s	53.0	54.9	57.4	60.0

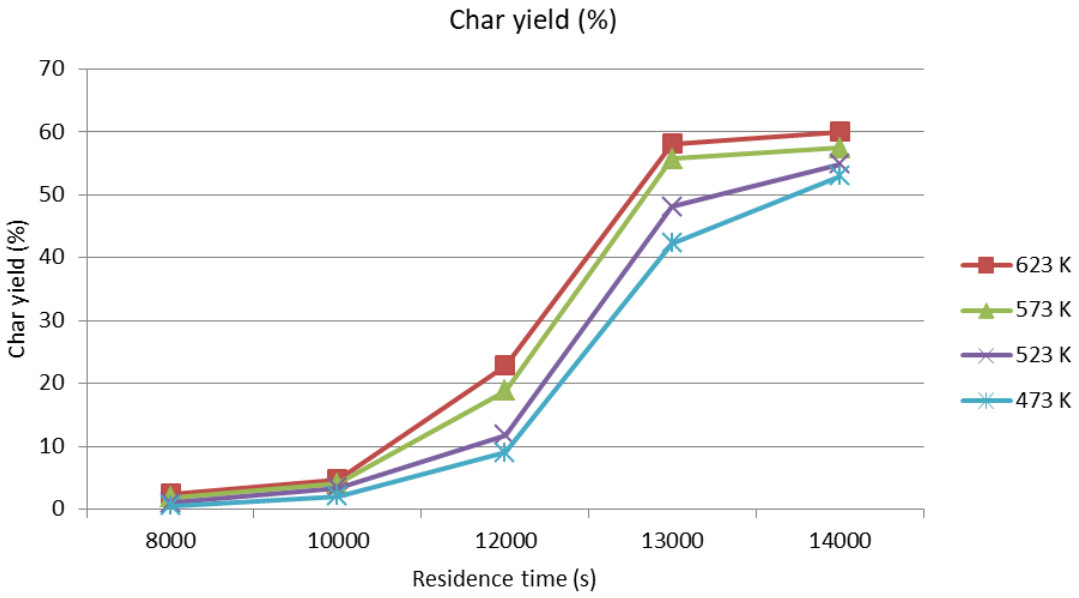

Figure 4- 3: Char yield percentage in outlet for different temperatures and residence times

Table 4- 6: Ash percentage in outlet for different temperatures and residence times

Temperature / R. Time	473K	523K	573K	623K
8000s	0.4	0.4	0.5	0.6
10000s	1.2	1.3	1.5	1.6
12000s	4.6	5.3	7.2	8.1
13000s	14.5	15.8	19.1	22.5
14000s	29.0	30.0	31.6	34.3

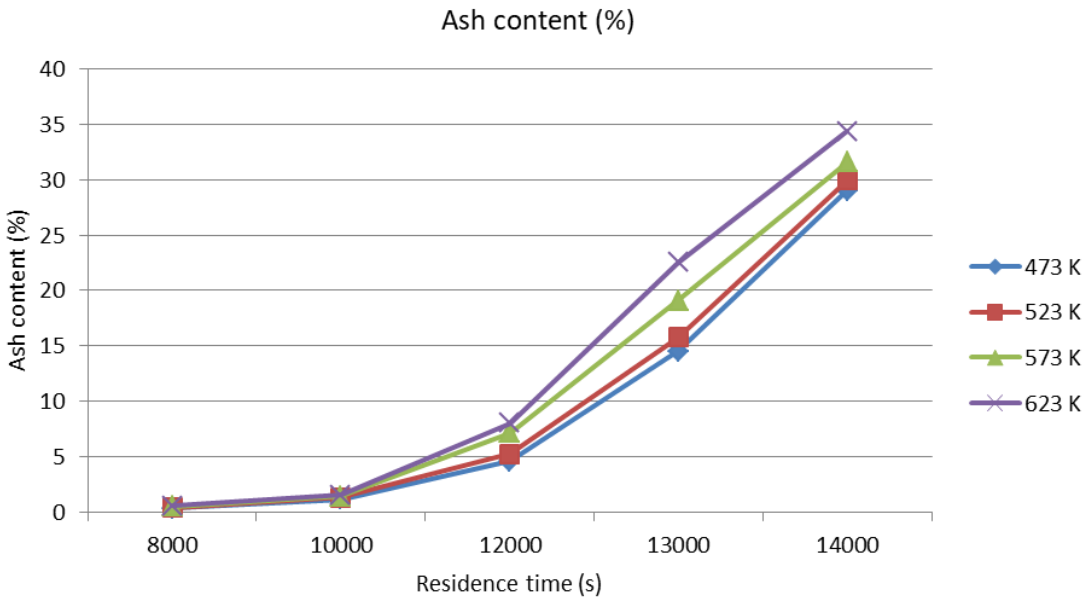

Figure 4- 4: Ash percentage in outlet for different temperatures and residence times

Table 4- 7: Unreacted lignocellulose percentage in outlet for different temperatures and residence times

Temperature / R. Time	473K	523K	573K	623K
8000s	97.7	97.1	96.0	95.4
10000s	96.3	94.8	93.9	93.2
12000s	86.1	82.7	73.6	68.8
13000s	42.9	35.9	24.8	19.0
14000s	17.8	14.9	10.8	5.5

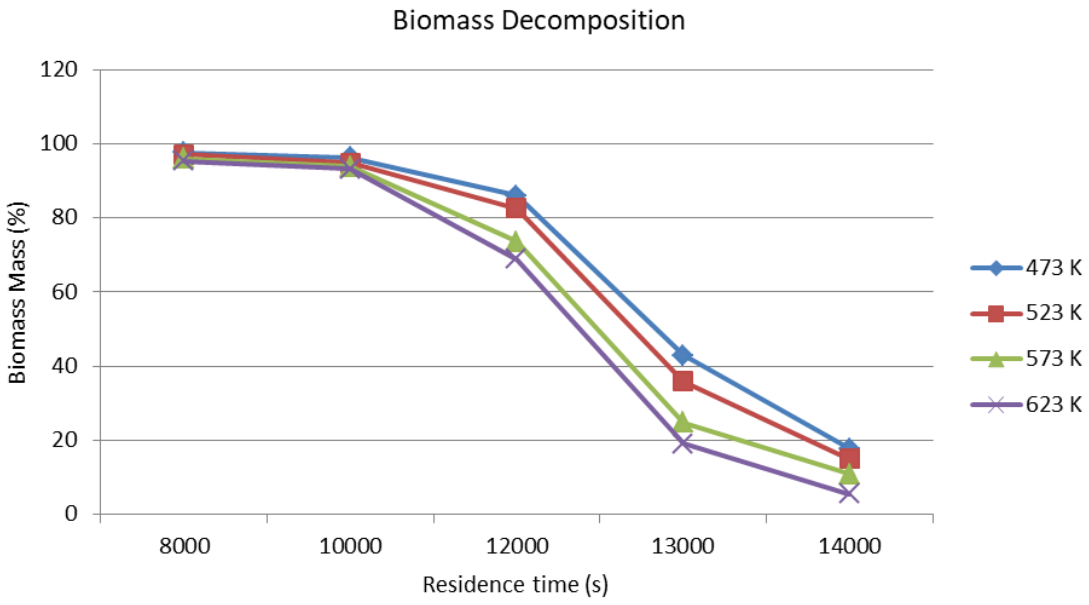

Figure 4- 5: Unreacted lignocellulose percentage in outlet for different temperatures and residence times

For all gas inlet temperatures, at 8000s residence time, char yields are less than 2.5% and biomass mass percentages in the solid outlet are in the range 95-100% which indicates that lignocellulose decomposition is at its initial phase and residence time 8000s is not sufficient for the temperatures in subject. Further referring to the simulations results for moisture content given in the figure 4-6, it can be noticed that drying process is completed for all gas inlet temperatures between 3000 – 5000s. As with the increase of residence time to 10000 s, lignocellulose decomposition has slowly progressed for all gas inlet temperatures giving rise to char yields in between 2-5%, which means an insufficient residence time for temperatures in subject.

This is mainly as a result of solid phase not being achieved high enough temperature for sufficiently longer time to activate and progress with the decomposition reactions. Referring to the solid temperature profiles given in the table 4-1, it can be concluded that both solid and gas phase temperatures are in the transient phase until 12000s.

When residence time is further increased to 12000s and then to 13000s, lignocellulose decomposition has been accelerated proportionally. In parallel with the biomass decomposition, char and ash generation also have accelerated. Residence time is again increased to 14000s and it is observed that acceleration of biomass decomposition is drastically reduced for 573K and 623K inlet gas temperatures while there is gradual decrease for both 473K and 523K inlet gas temperatures. This is mainly due to the very low concentration of available unreacted biomass. For all gas inlet temperatures, at 14000s residence time, ash content is very high in the outlet as it ranges between 29-35%. This is mainly due to the fact that generated char is extensively being utilized in heterogeneous reactions at elevated temperatures.

Since biochar production is the main objective of this study, optimized gas inlet temperature and residence time are determined accordingly based on the char yield, ash content and unreacted biomass content. Therefore optimized gas inlet temperature and residence time are identified as 573K and 13000s and respective char yield is 55.7%. For 573K and 13000s residence time, drying is completed within 4000s as depicted in figure

4-6. In addition, process of lignocellulose decomposition is depicted in the figure 4-8 as unreacted lignocellulose composition profiles over the time span for the optimized conditions of gas inlet temperature 573K and residence time 13000s.

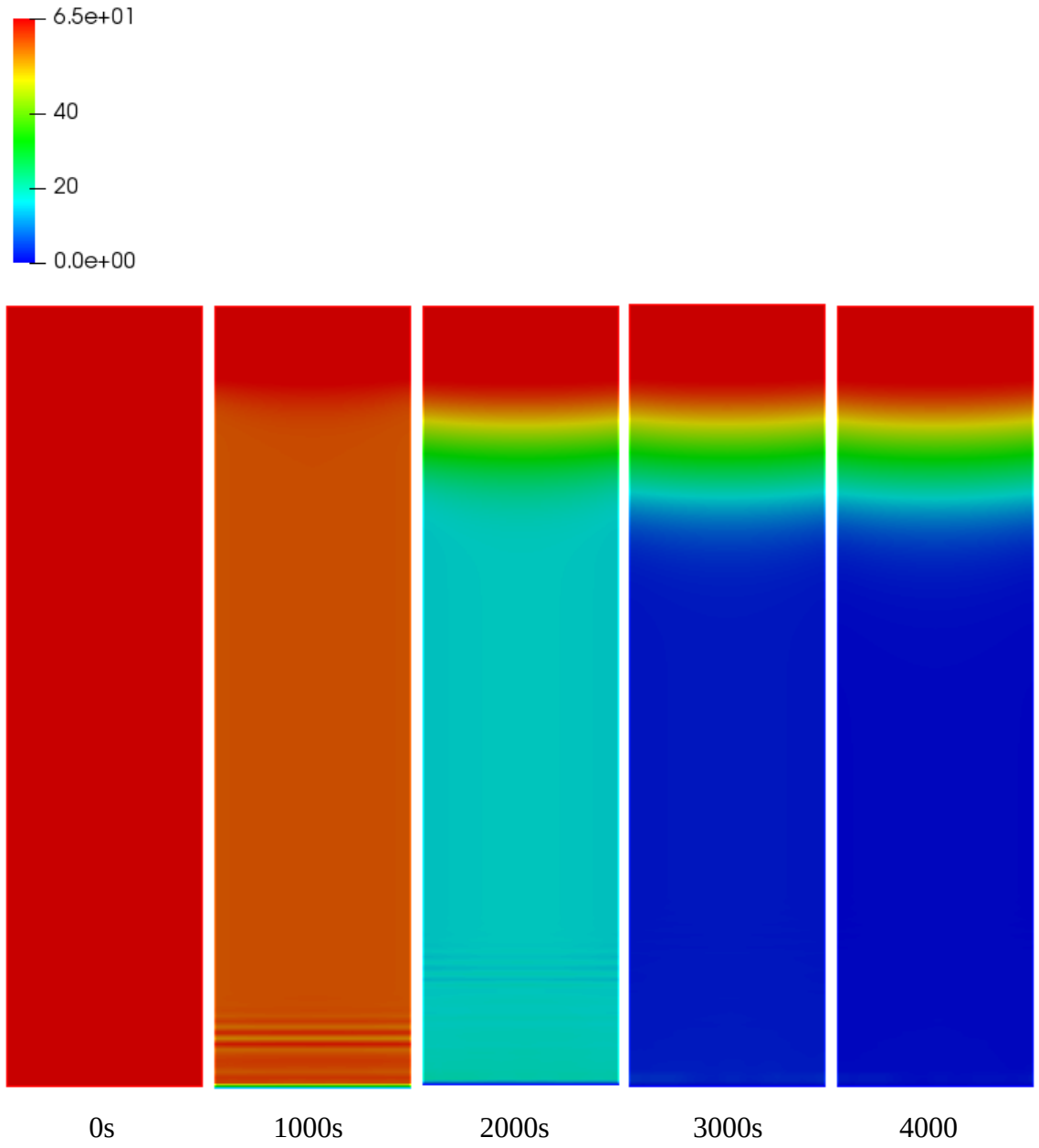

Figure 4- 6: Moisture content profiles over the time for optimized case (573K, 14000s)

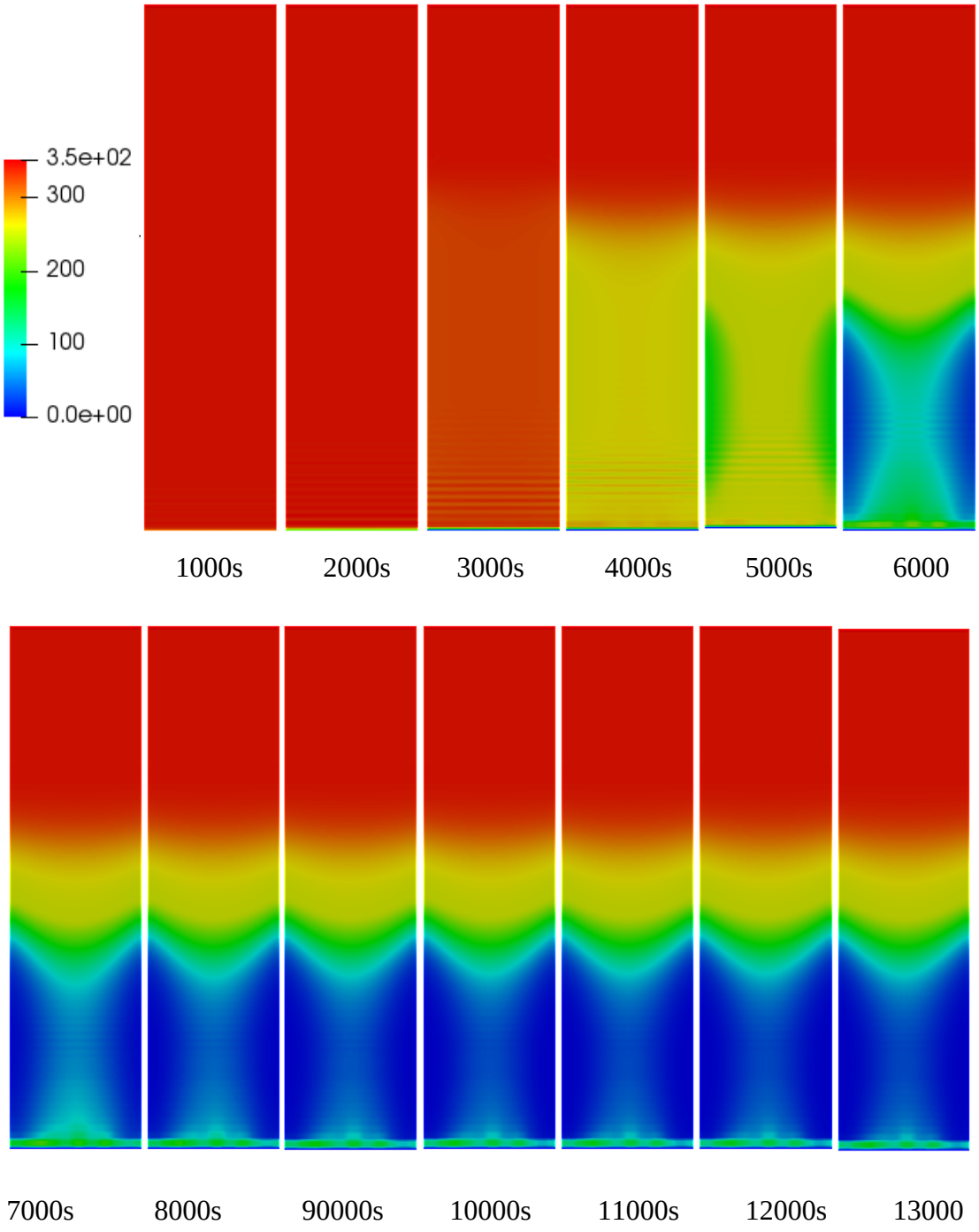

Figure 4- 7: Profiles of unreacted lignocellulose per unit volume over the time span for optimized case (573K, 13000s)

4.3 Optimization of geometry

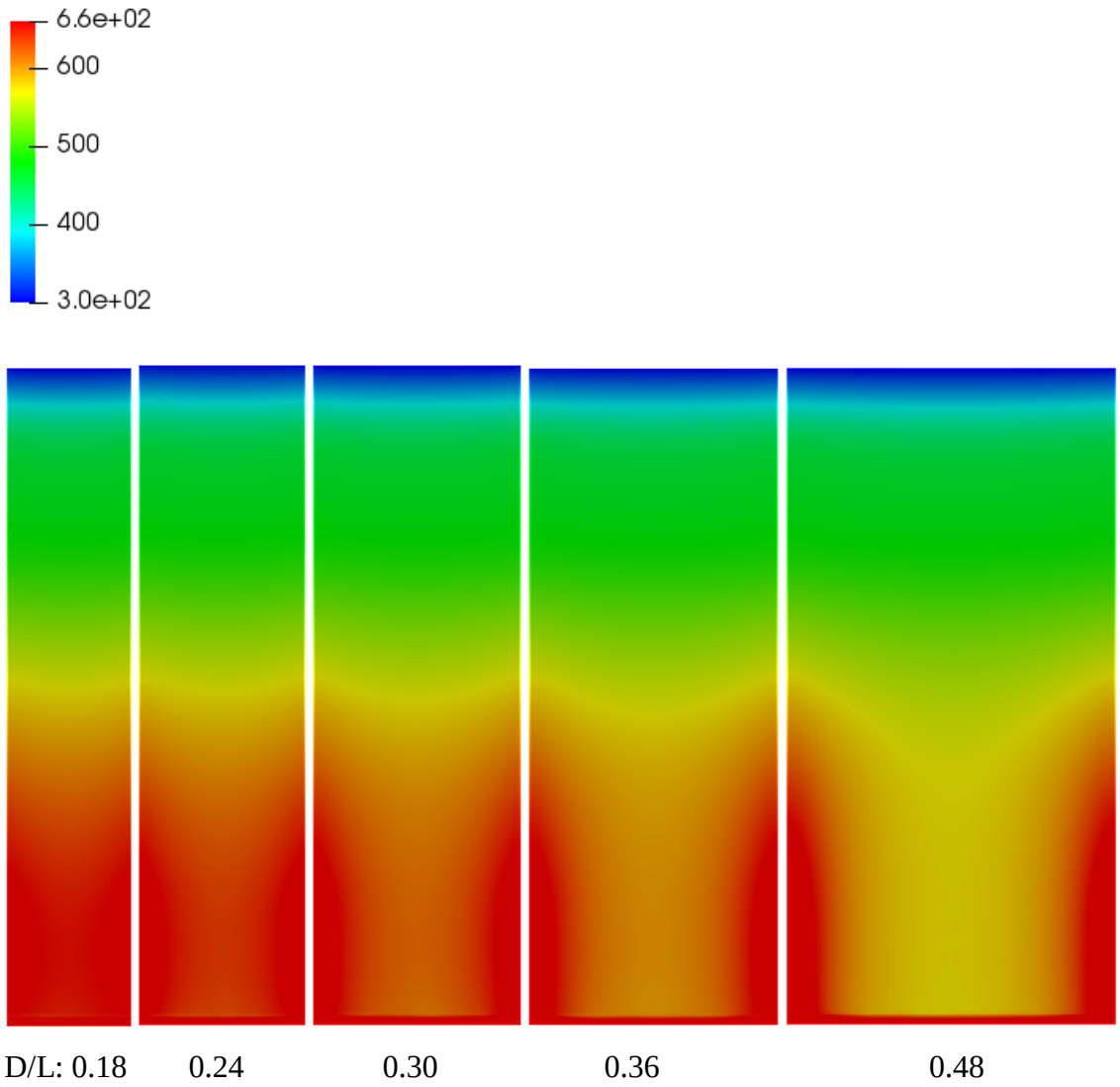

Figure 4- 8: Solid temperature profiles for different D/L ratios at optimized conditions

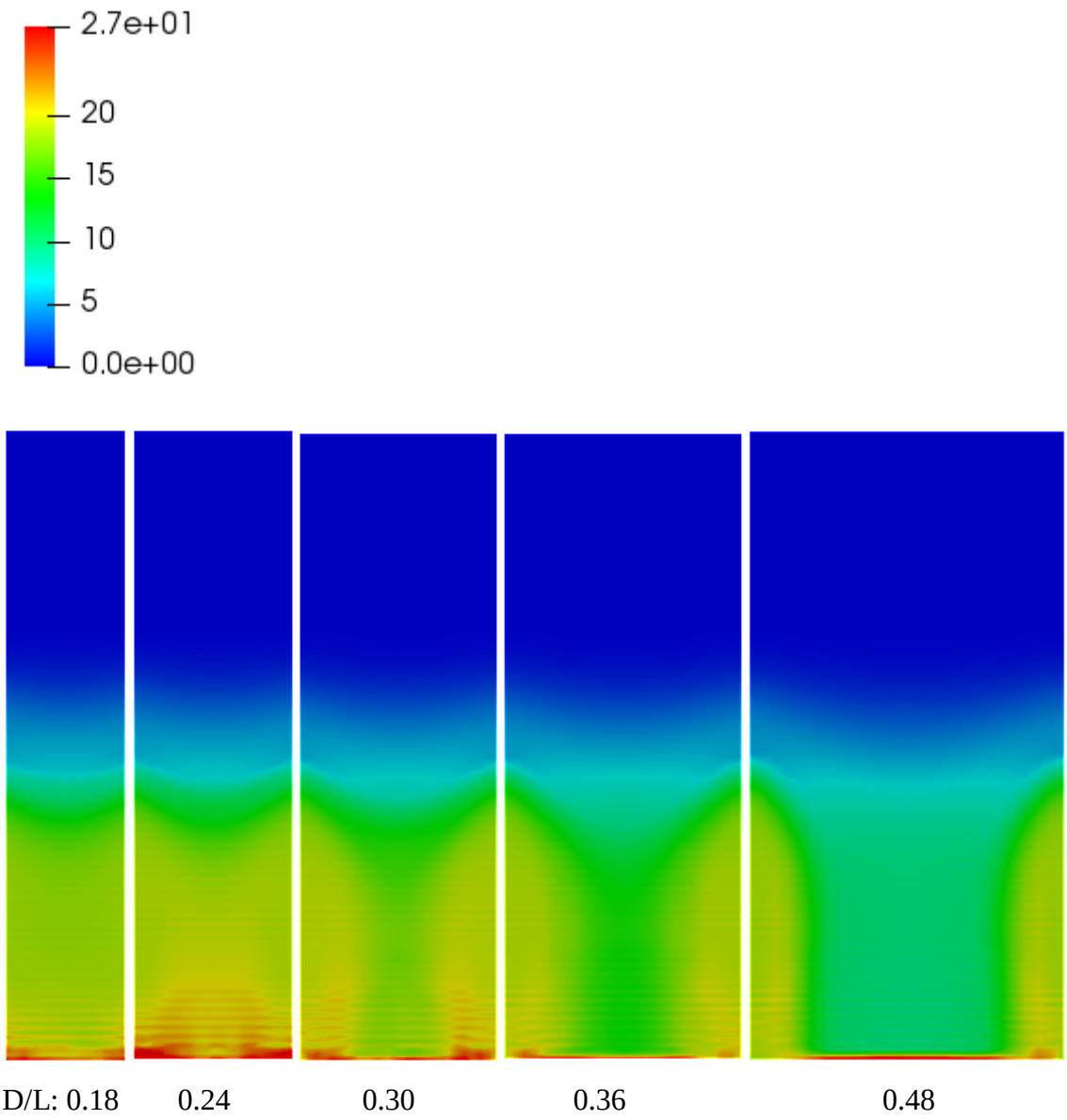

Figure 4- 9: Char yield profiles for different D/L ratios at optimized conditions

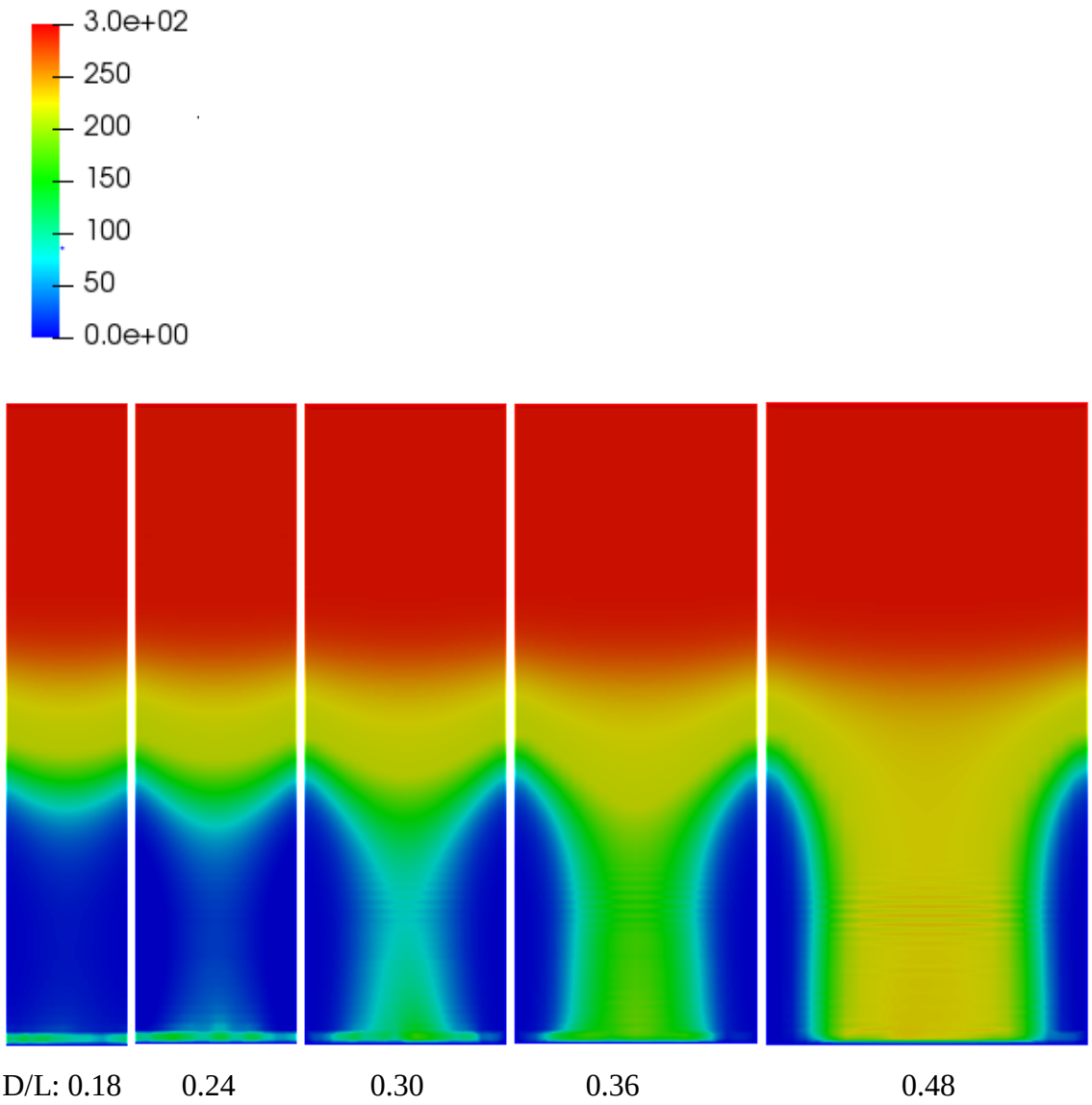

Figure 4- 10: Unreacted lignocellulose composition profiles for different D/L ratios at optimized conditions

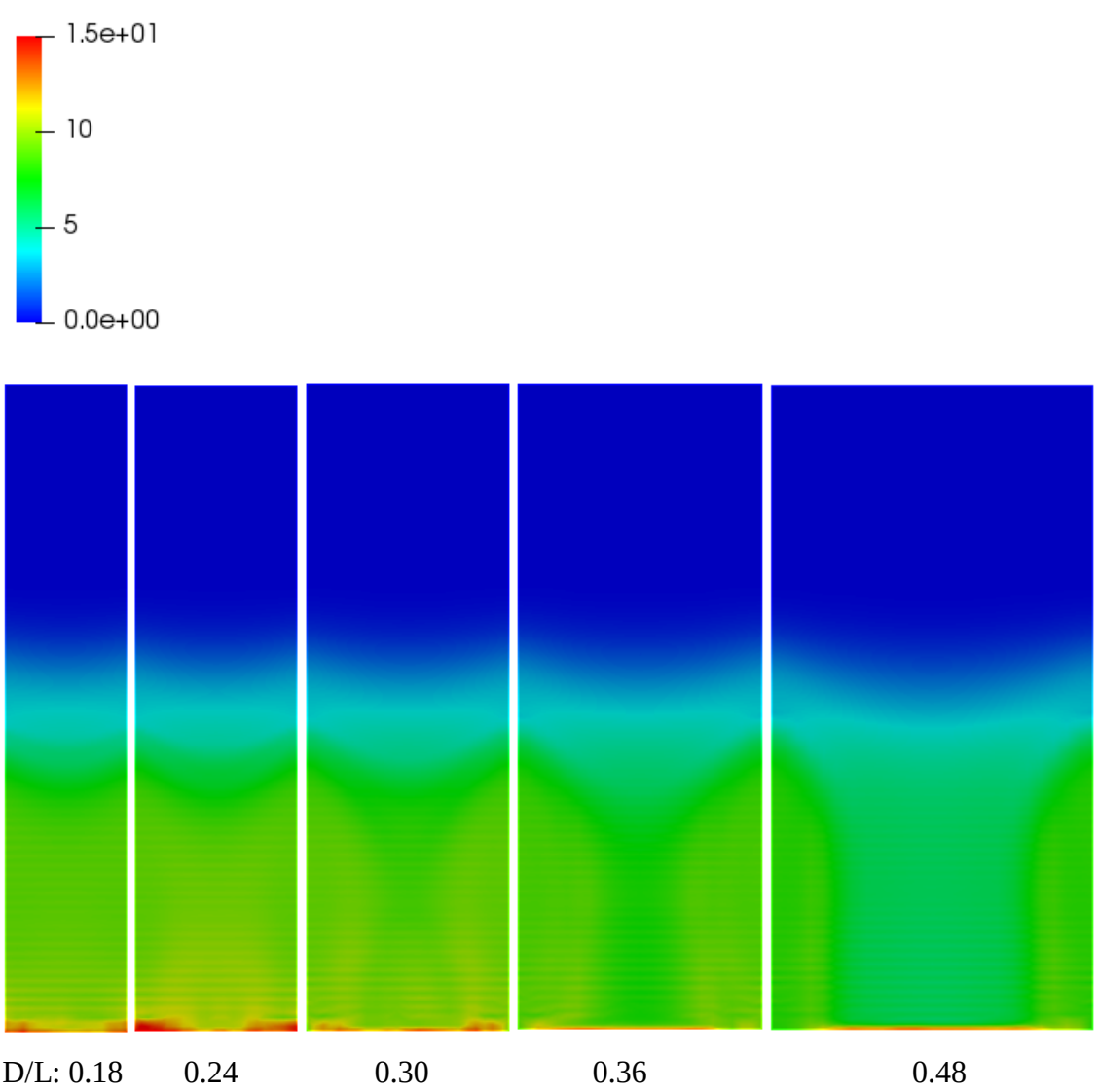

Figure 4- 11: Ash content per unit volume profiles for different D/L ratios at optimized conditions

Table 4- 8: Char, ash and unreacted lignocellulose percentages in the outlet with respect to D/L ratio

Component / D/L	Char %	Ash %	Unreacted lignocellulose %
0.18	57.3	29.1	13.4
0.24	55.7	19.1	24.8
0.3	23.8	10.0	66.2
0.36	13.5	5.0	81.5
0.48	5.3	2.3	92.3

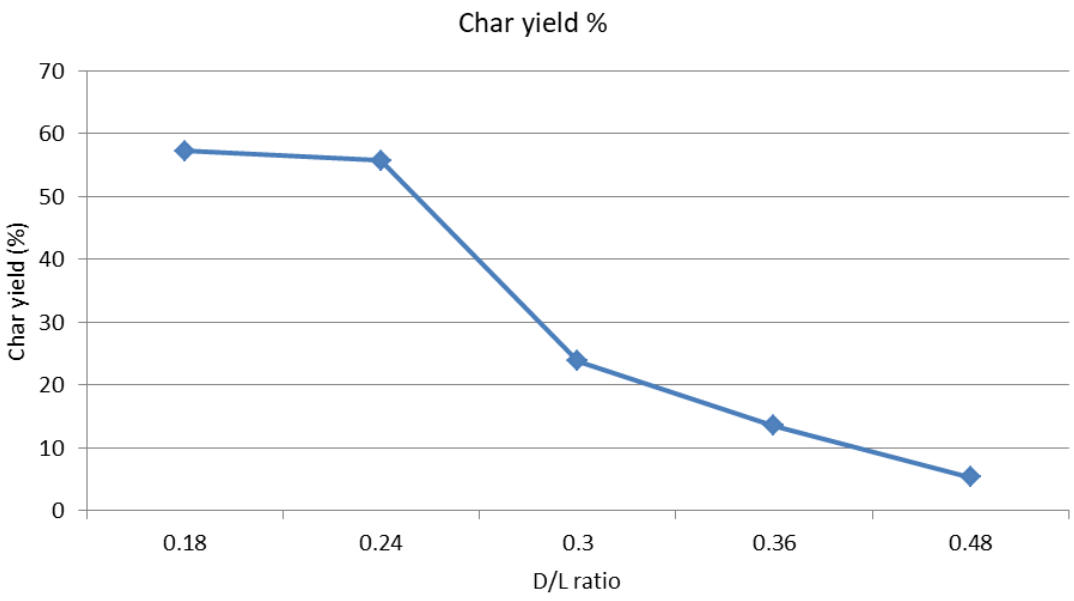

Figure 4- 12: Char percentage in the outlet with respect to D/L ratio

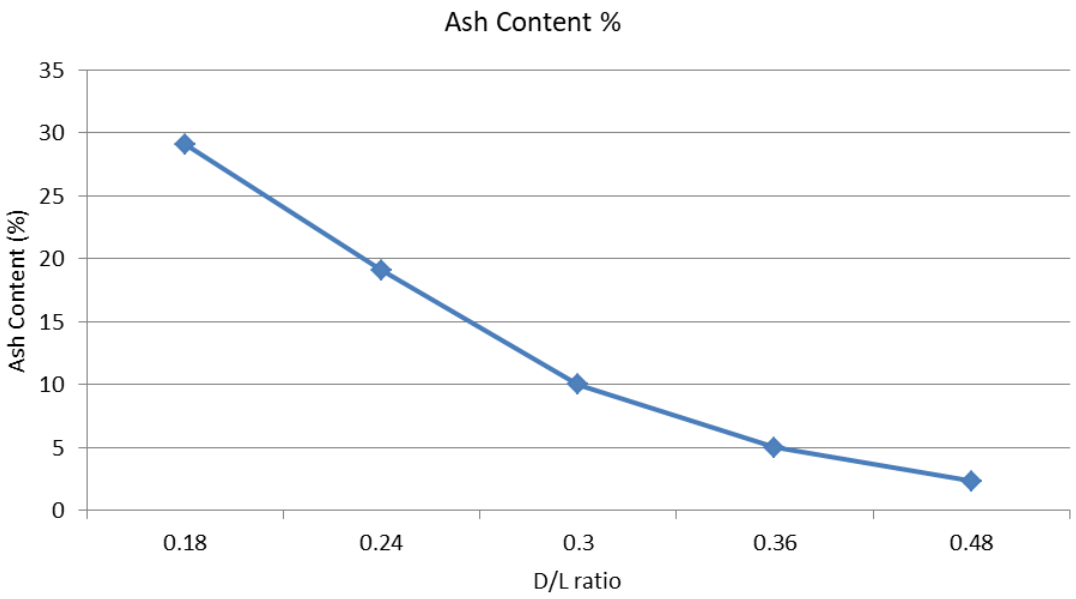

Figure 4- 13: Ash percentage in the outlet with respect to D/L ratio

According to the above results, as D/L ratio increases, char yield decreases for optimum gas inlet temperature and residence time (573K, 13000s). However for D/L ratios 0.18 and 0.24, difference of char yields is not significant but ash content is significantly higher for the former. Therefore optimum D/L ratio for a cylindrical reactor for the previously determined optimum gas inlet temperature and residence time is 0.24.

Given below in the table 4-8 and table 4-9 are respectively exit gas and exit solid compositions for the optimum conditions (T_g: 573K, Residence time: 13000s and D/L: 0.24).

Table 4- 9: Exit gas composition at the gas outlet for the optimum conditions

Gas component	Composition (w/w%)
CO_2	20.38
H_2O	17.83
CO	2.37
H_2	0.34
CH_4	0.21
O_2	0.31
N_2	58.56

Table 4- 10: Solid composition at the solid outlet for the optimum conditions

Component	Composition (w/w%)
Char	55.7
Ash	19.1
Unreacted biomass	24.8
Moisture	0.4

4.4 Biochar quality and suitability for an industrial application

The quality of biochar produced depends on many parameters such as fixed carbon content, C/O & C/H ratio, pH, bulk density, moisture content, specific surface area, hydrophilicity, nutrient contents (N,P & K) and heavy metal contents. In fact, for an accurate and complete quality analysis, produced biochar samples should be tested for above parameters experimentally. Depending on the porosity and absorption capacities, this biochar has a great potential to be used in landfill leachate treatment.

4.5 Model validation

Since the solid velocities employed in this continuous packed-bed reactor model are very small (0.00015 - 0.00025 ms^{-1}) and closer to zero, it may have negligible deviations in the vicinity range of solid velocity 0 – 0.00025 ms^{-1}. Experimental reactor set-up is made similar to the application in subject where hot gas enters from the bottom and the solid velocity is zero. In this experimental reactor set-up, four thermocouples are installed along the center line of the height of the experimental packed-bed reactor so that experimental data for temperature profiles can be compared with the simulation results of solid and gas phase temperatures for same physical and operating conditions as given in the table 4-10. The simulation results are in good agreement with experimental data as average deviation from the experimental data is 3.75%. The experimental setup is a cylindrical reactor whose height and diameter is respectively 1.2m and 0.35m. Thermocouples are installed 0.2m, 0.4m, 0.6m and 0.9m away from the bottom of the reactor along the center line.

Table 4- 11: Operating parameters of the experimental reactor

Parameter	Value
Gas flow rate	6 m^3/h
Simulation time	2700s
Solid velocity	0 ms^{-1}
Solid inlet temperature	300 K

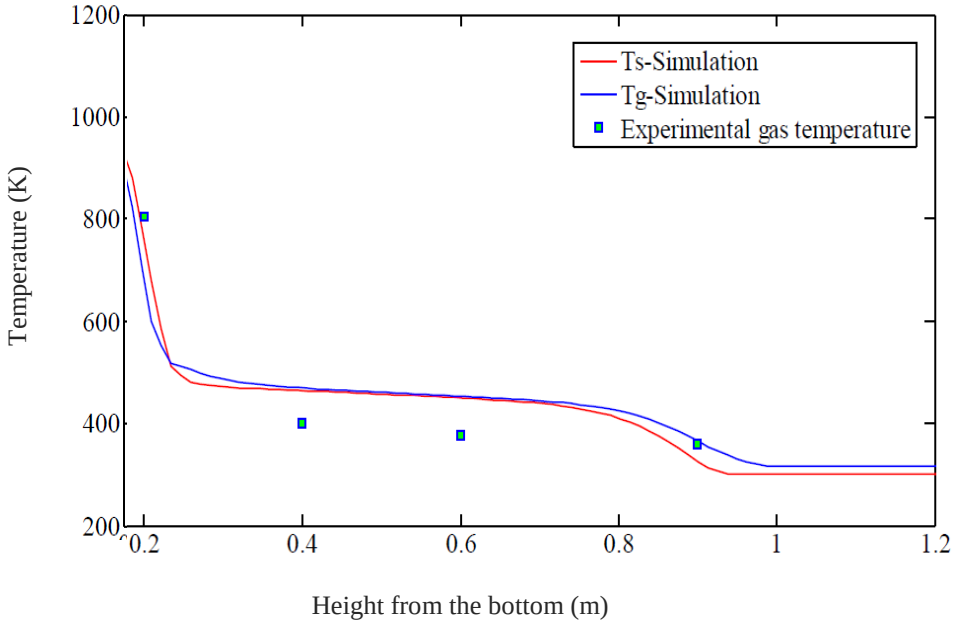

Figure 4- 14: Simulation and experimental temperature profiles after 2700s

The developed model is further validated for biomass mass reduction by using a fixed-bed of biomass. As similar to the previous validation, use of a fixed-bed of biomass may have negligible deviation from the simulated process since the solid velocities employed in the simulations are very small. The experimental reactor is in dimensions of 0.2m diameter and 0.2m height. In the validation, biochar yield and experimental mass loss data based on the initial mass of biomass is compared with the simulation results. Experimental conditions are given in the following table 4-11. Experimental mass loss is 95.4% and results are in good agreement with the simulation results as average deviation from the experimental mass loss is under 1%.

Table 4- 12: Operating parameters of the experimental reactor

Parameter	Value
Inlet gas temperature	623 K
Inlet gas composition	N_2 – 100%
Inlet gas velocity	1.5 ms^{-1}
Solid velocity	0 ms^{-1}
Solid inlet temperature	300 K

5. CONCLUSIONS

The mathematical model developed in this study for the torrefaction of composted organic MSW, was converted to a numerical model and simulated by OpenFOAM. The developed model is in good agreement with the actual process which is assured by the validation process. Following conclusions are made via the results and analysis.

- Solid and gas phase temperature gradually become steady after 13000s and residence times less than 13000s for gas inlet temperatures in subject (473K, 523K, 573K and 623K) are not sufficient for a complete torrefaction process and hence result lesser char yield. In addition, there exists a high temperature zone in neighboring region of the bottom part of the reactor wall which is caused by an increase of heat transfer occurred between gas and solid phase due to low gas velocities in the region.
- Ash content in the outlet gradually increases with the residence time for all gas inlet temperatures in subject up to 12000s. Increase in ash content is rapid for residence times higher than 13000s. This is a result of extended torrefaction reactions and also generated char being utilized in combustion and gasification reactions.
- Optimum residence time and gas inlet temperature for the torrefaction process are respectively 13000s and 573K.
- Optimum D/L ratio for a cylindrical reactor is 0.24 and hence the optimum dimensions for the torrefaction reactor are height of 2m and diameter of 0.48m.
- Biochar yield for the optimum conditions and geometry is 55.7% while ash content in the outlet is 19.1%. In dry basis, 95.9% of biomass has been decomposed. Total weight loss based on the initial wet biomass is 86.6%.

5.1 Drawbacks of the model and suggestions for future works

- As the torrefaction progresses, particle size reduces during the period of residence time as a function of temperature, time and mass fractions of char, ash

and lignocellulose. The developed model is not incorporated with the particle size reduction model and hence the results may have been slightly impacted by that. Semi-empirical model developed through experimental data for the subjective application may need to be included to further improve the accuracy. The relevant data required to develop the semi-empirical model can be obtained during the pilot-scale operation.

- Though the developed OpenFOAM numerical model is included with a turbulence model, simulations are run assuming laminar flow conditions due to the slow flow rates associated with the application. Therefore the same model can be used to simulate a torrefaction system with different turbulence conditions. In order to do that, specific k and ε (turbulent kinetic energy and turbulent dissipation rate) values need to be determined experimentally.
- In this torrefaction model, solid porosity and sphericity variations are assumed to be of negligible impact and hence the model is not included with a model for solid porosity variation. Any impact caused otherwise may eliminated by incorporating a specific solid porosity variation model for the application. Such a model can be accurately developed as a semi-empirical model via an experimental approach.
- In this torrefaction model, solid velocity gain due to the bed shrinkage is neglected assuming that associated solid velocities are high enough to not consider such velocity gains. For a higher accuracy, a bed shrinkage model may be combined with this model.
- The developed model can be further enhanced by incorporating advanced reaction kinetics which include both primary and secondary torrefaction reactions, tar formation reactions and heterogeneous reactions.
- The developed model can be modified to simulate and optimize various biomass torrefaction systems without limiting to composted organic MSW of this particular application.

REFERENCES

[1] Peter McKendry, "Energy production from biomass (part 1): overview of biomass," *Bioresource Technology*, vol. 83, pp. 37-66, 2002.

[2] Tomoaki Namioka, Kunio Yoshikawa Kentaro Umeki, "Analysis of an updraft biomass gasifier with high temperature steam using," *Applied Energy*, vol. 90, pp. 38-45, 2012.

[3] "WBA Global Bioenergy Statistics 2018," World Bioenergy Association, Summery Report 2018.

[4] Perinaz Bhada-Tata Daniel Hoornweg, "WHAT A WASTE, A Global Review of Solid Waste Management," Urban Development & Local Government Unit, World Bank, 2012.

[5] "Annual Report 2012," Central Environmental Authority, Sri Lanka, Annual Report 2012.

[6] Peter McKendry, "Energy production from biomass (part 2): conversion technologies," *Bioresource Technology*, vol. 83, pp. 47-54.

[7] Y. Neubauer, "Biomass Gasification," in *Biomass Combustion Science, Technology and Engineering*, Lasse Rosendahl, Ed.: Woodhead Publishing Limited, 2013, ch. 6, pp. 106-129.

[8] A. Bridgwater, "Fast pyrolysis of biomass for the production of liquids," in *Biomass Combustion Science, Technology and Engineering*, Lasse Rosendahl, Ed.: Woodhead Publishing Limted, 2013, ch. 7, pp. 130-171.

[9] V. Nallathambi Gunaseelan, "Anaerobic Digestion of Biomass for Methane Production," *Biomass and Bioenergy*, vol. 13, pp. 83-114, 1997.

[10] Yunbo Zhaia, Yun Zhuc, Caiting Lia, Guangming Zeng Tengfei Wanga, "A review of the hydrothermal carbonization of biomass waste for hydrochar formation: Process conditions, fundamentals, and physicochemical properties," *Renewable and Sustainable Energy Reviews*, vol. 90, pp. 223-247, 2018.

[11] J. Patrick A. Hettiaratchi, S. C. Wirasinghe, Sumith Pilapiiya Nilanthi J. G. J. Bandara, "Relation of waste generation and composition to socio-economic factors: a case study," *Enviornmental Monitering and Assessment*, vol. 135, pp. 31-39, 2007.

[12] Florian Hoffmann, Bernhard Peters Amir Houshang Mahmoudi, "Application of XDEM as a novel approach to predict drying of a packed bed," *International Journal of Thermal Sciences*, vol. 75, pp. 65-75, 2014.

[13] Mahinsasa Narayana Niranjan Fernando, "A comprehensive two dimensional Computational Fluid Dynamics model for an updraft biomass gasifier," *Renewable Energy*, vol. 99, pp. 698-710, 2016.

[14] M. Vascellari, G. Cau S. Murgia, "Comprehensive CFD model of an air-blown coal-fired updraft gasifier," *Fuel*, vol. 101, pp. 129–138, 2012.

[15] Qinglin Zhang, Weihong Yang, Wlodzimierz Blasiak Yueshi Wu, "A two-dimensional CFD simulation of biomass gasification in a downdraft fixed bed gasifier with highly preheated air and steam," *Energy Fuels*, May 2013.

[16] W Malalasekera H K Versteeg, *An Introduction to Computational Fluid Dynamics*, 2nd ed.: Pearson Education Limited, 2007.

[17] Andrzej BIAŁOWIEC Paweł STĘPIEŃ, "Mathematical Modelling of Wooden Biomass torrefaction," *Drewno*, vol. 60, pp. 51-65, 2017.

[18] Michael P. Twedt, Christina Gerometta, Evan Almberg Stephen Gent, "Fundamental Theories of Torrefaction by Thermochemical Conversion," in *Theoretical and Applied Aspects of Biomass Torrefaction*.: Elsevier Inc., 2017, ch. 3, pp. 41-75.

[19] Radu Godina, João Carlos de Oliveira Matias, Leonel Jorge Ribeiro Nunes Jorge Miguel Carneiro Ribeiro, "Future Perspectives of Biomass Torrefaction: Review of the Current State-Of-The-Art and Research Development," *Sustainability*, vol. 10, July 2018.

[20] Peter Quickerb Kathrin Webera, "Properties of biochar," *Fuel*, vol. 217, pp. 240-261, 2018.

[21] Arjen Boersma, Robin Zwart, J. H. A. Kiel P.C.A. Bergman, "Torrefaction for Biomass Co-Firing in Existing Coal-Fired Power Stations," Energy research Centre of the Netherlands, ECN Report 2005.

[22] J Carlos De Oliveira Matias, J P Da Silva C Leonel Jorge Ribeiro Nunes, "Biomass Torrefaction Process," in *Torrefaction of Biomass for Energy Application*.: Elsevier Inc, 2017, ch. 3, pp. 89-124.

[23] Krzysztof J. Ptasinski, Frans J.J.G. Janssen Mark J. Prins, "Torrefaction of wood: Part 1. Weight loss kinetics," *Journal of Analytical and Applied Pyrolysis*, vol. 77, pp. 28-34, 2006.

[24] Krzysztof J. Ptasinski, Frans J.J.G. Janssen Mark J. Prins, "Torrefaction of wood: Part 2. Analysis of products," *Journal of Analytical and Applied Pyrolysis*, vol. 77, pp. 35-40, 2006.

[25] James R. Arcate, and Thomas B. Reed Edward S. Lipinsky, "Enanced Wood Fuels via Torrefaction," *Division of Fuel chemistry*, vol. 47, pp. 408-410, 2002.

[26] J Carlos De Oliveira Matias, J P Da Silva C Leonel Jorge Ribeiro Nunes, "Applications for Torrefied Biomass," in *Torrefaction of Biomass for Energy Application*.: Elsevier Inc., 2017, ch. 11, pp. 203-214.

[27] JianqiaoWang, Yijun Pan, Boxiong Shena, ChunfeiWub Peng Yuan, "Reviewof biochar for themanagement of contaminated soil: Preparation, application and prospect," *Science of the Total Environment*, vol. 659, pp. 473–490, 2019.

[28] I. Malgarinos, N. Nikolopoulos, P. Grammelis, S. Karrelas, E. Kakaras A. Nikolopoulos, "A decoupled approach for NOx–N2O 3-D CFD modeling in CFB plants," *Fuel*, vol. 115, pp. 401-415, 2014.

[29] A. Jhalani, M. R. Ravi, A. Ray S. Sinha, "Modelling of Pyrolysis in Wood: A Review," *SESI Journal*, vol. 10, pp. 41-62, 2000.

[30] W. A. M. K. P. Wickramaarachchi, Mahinsasa Narayana Muhammad Amin, "Performance Analysis of Updraft Gasifier," in *International Conference on Sustainable Energy Engineering and Application (ICSEEA)*, 2016, pp. 61-65.

[31] I. Obernberger, F. Biedermann C. Mandl, "Modelling of an updraft fixed-bed gasifier operated with softwood pellets," *Fuel*, vol. 89, pp. 3795-3806, 2010.

[32] M. Narayana K.U.C. Perera, "Finite Volume Analysis of Biomass Particle Pyrolysis," in *Moratuwa Engineering Research Conference (MERCon)*, 2017, pp. 379-384.

[33] J.A. van Oijen, L.P.H. de Goey Y. Haseli, "A detailed one-dimensional model of combustion of a woody biomass particle," *Bioresource Technology*, vol. 102, pp. 9772–9782, 2011.

[34] Mahinsasa Narayana Niranjan Fernando, "A comprehensive two dimensional Computational Fluid Dynamics model for an updraft biomass gasifier," *Renewable*

Energy, vol. 99, pp. 698-710, 2016.

[35] Hui Liu, "CFD Modeling of Biomass Gasification Using a Circulating Fluidized Bed Reactor," University of Waterloo, Ontario, Canada, PhD Thesis 2014.

[36] Lamees Akawi, Murray Moo-Young, C. Perry Chou Kajan Srirangan, "Towards sustainable production of clean energy carriers from biomass resources," *Applied Energy*, vol. 100, pp. 172–186, 2012.

[37] Xi Gao, Ya-ping Zhu, Zheng-hong Luo Ya-Qing Zhuang, "CFD modeling of methanol to olefins process in a fixed-bed reactor," *Powder Technology*, vol. 221, pp. 419–430, 2012.

[38] R.E. treybal, *Mass transfer Operations*, 3rd ed.: McGraw-Hill Book company, 1980.

[39] Tomáš Juˇrena, "NUMERICAL MODELLING OF GRATE COMBUSTION," Brno University of Technology, PhD Thesis 2012.

[40] Pawel Jan Zukb, Konrad Bajera, Marek Dudynski Kamil Kwiatkowskia, "Biomass gasification solver based on OpenFOAM," *Computer Physics Communications*, 2013.

APPENDICES

Appendix A

Table A- 1: Gas-phase temperature (Tg) profiles

	473 K	523 K	573 K	623 K
8000 s	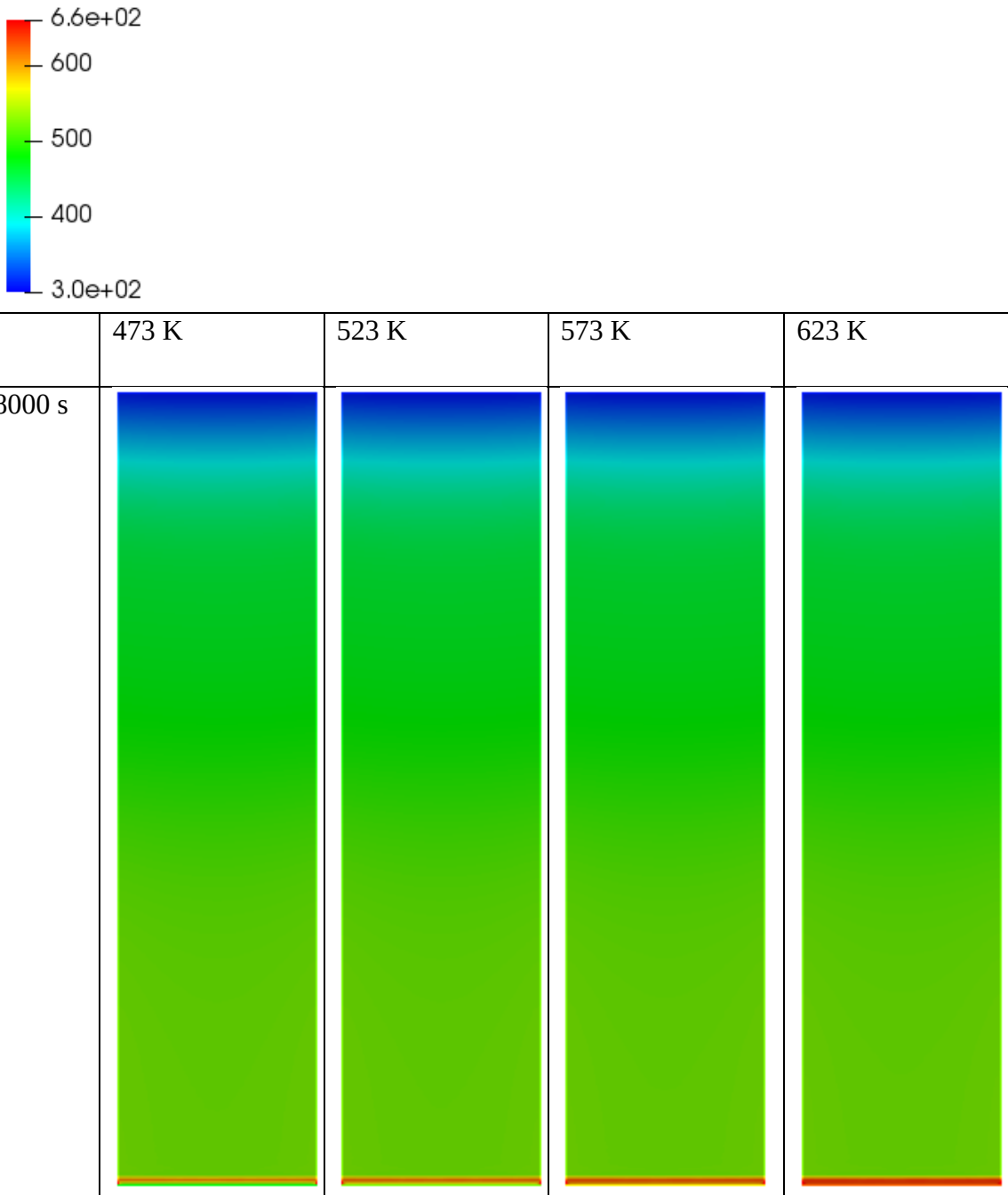			

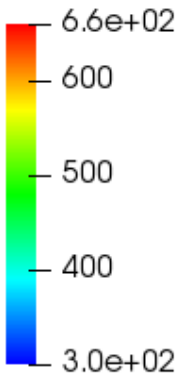

	473 K	523 K	573 K	623 K
10000 s				

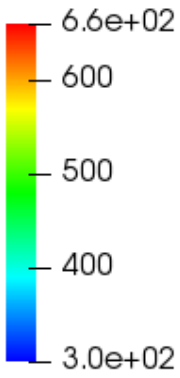

	473 K	523 K	573 K	623 K
12000 s				

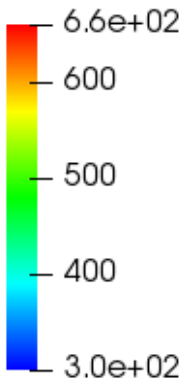

	473 K	523 K	573 K	623 K
13000 s				

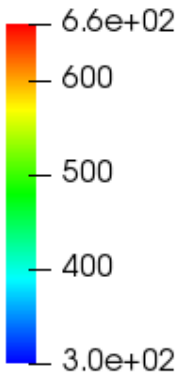

	473 K	523 K	573 K	623 K
14000 s				